

# Development of FESTR: a new spectroscopic modeling and analysis code

Peter Hakel

Los Alamos National Laboratory

October 6, 2015

2015 National ICF Diagnostics Working Group Meeting  
Los Alamos National Laboratory

# Acknowledgements

---

- Atomic physics and opacity
  - XCP-5: C. Fontes, T. Joshi
  - T-1: J. Colgan, H. Johns, D. Kilcrease, M. Sherrill
  - T-4: E. Timmermans, ...  
(H.L. Zhang, R.E.H. Clark, G. Csanak, R.D. Cowan, D. Sampson, J. Abdallah, N. Magee)
- DIME (... – 2014)
  - M. Schmitt\*, S. Hsu\*, P. Bradley\*, G. Kyrala, R. Shah, T. Murphy, J. Baumgaertel, I. Tregillis, N. Krasheninnikova, J. Cobble, S. Batha, R. Kanzleiter, ...
- KPE\* (2014 – ...)
  - H. Herrmann, Y. Kim, G. Kagan, A. McEvoy, N. Hoffman, ...

# Outline

---

- Motivation
- Implementation
- Examples
- Future work

# Outline

---

- Motivation
- Implementation
- Examples
- Future work

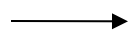
# Overview of LANL suite of atomic physics codes

---

- LTE and NLTE plasmas can be modeled
- Various levels of detail
  - Non-relativistic configuration average kinetics ( $nl^w$ ) + UTA spectra
  - Relativistic configuration average kinetics ( $nlj^w$ ) + UTA spectra
  - Mixed UTA (MUTA)
    - Configuration average kinetics
    - Spectra composed of mixture of UTAs and fine-structure features
  - Fine-structure levels
- NLTE rate matrix of max order  $\sim 10^7$  can be calculated

# The LANL Suite of atomic modeling codes

Atomic Physics Codes



Atomic Models

ATOMIC

CATS: Cowan Code

fine-structure  
config-average  
UTAs  
MUTAs

LTE or NLTE  
populations

RATS: relativistic

energy levels  
gf-values  
 $e^-$  excitation  
 $e^-$  ionization  
photoionization  
autoionization

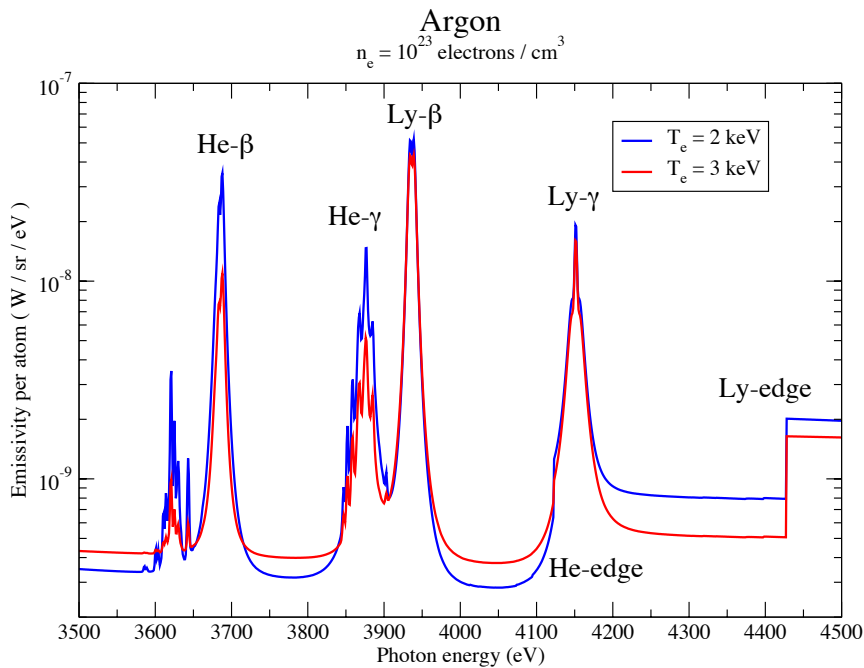
spectral modeling  
emission  
absorption  
transmission  
power loss

ACE:  $e^-$  excitation

GIPPER: ionization

<http://aphysics2.lanl.gov/tempweb>

# Examples of ATOMIC output (NLTE, uniform)

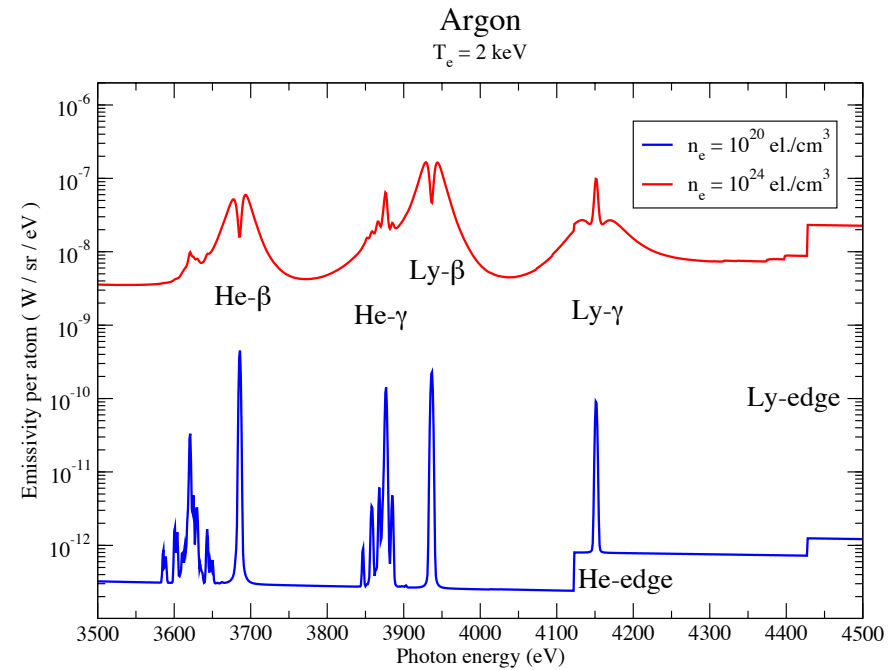
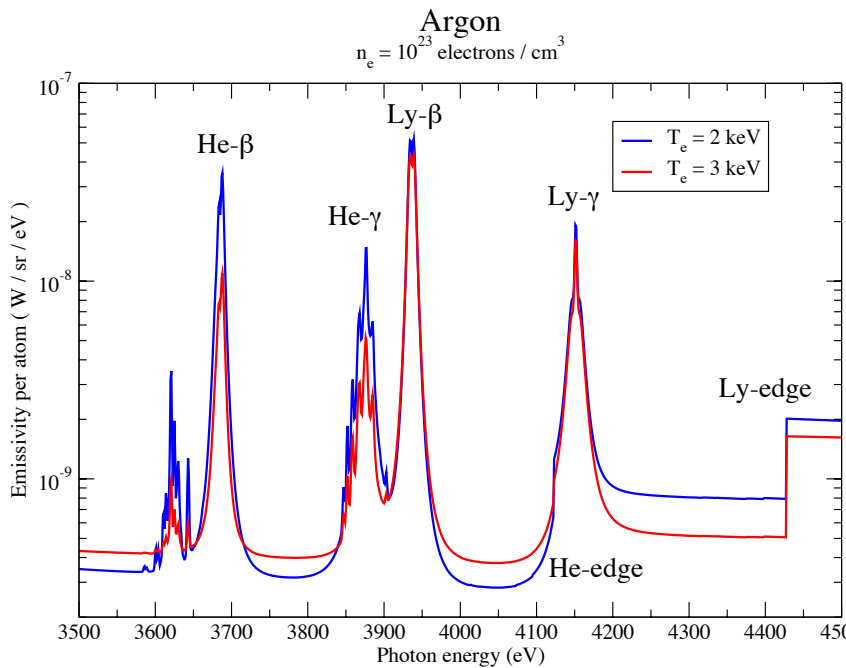


Argon charge-state populations:  
 $n_e = 10^{23}$  el. / cm<sup>3</sup>

	$T_e = 2$ keV	$T_e = 3$ keV
He-like	0.11	0.02
H-like	0.49	0.29
bare	0.40	0.69
$\langle Z \rangle$	17.3	17.7

Line intensities  
show sensitivity  
to electron temperature.

# Examples of ATOMIC output (NLTE, uniform)

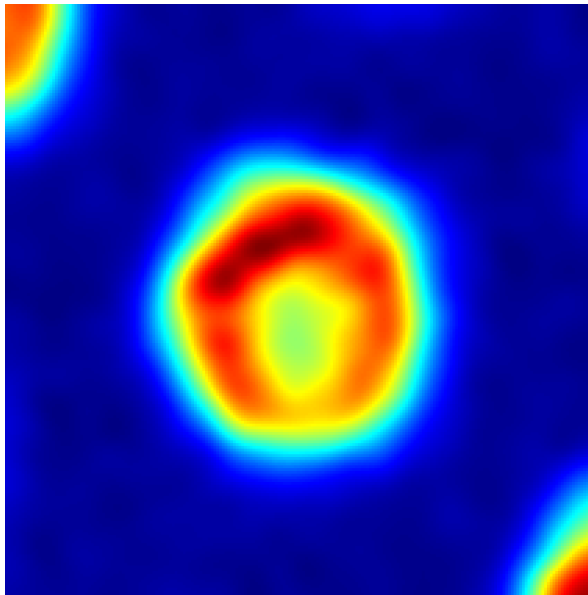


**Line intensities**  
show sensitivity  
to electron **temperature**.

**Line widths and shapes**  
show sensitivity  
to electron **density**.

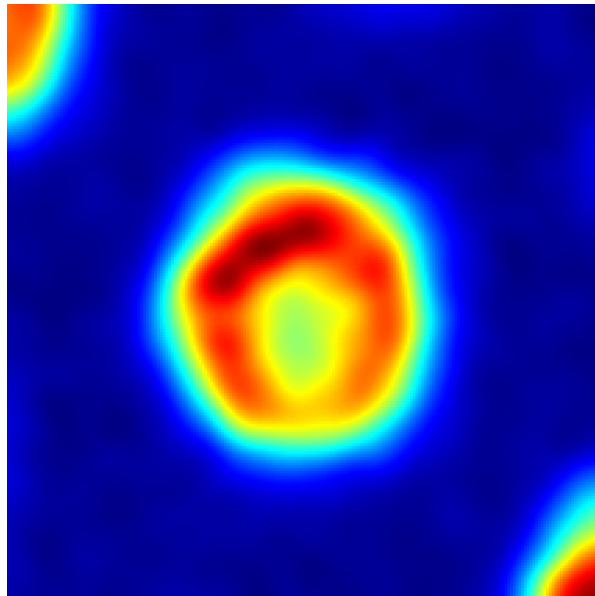
# Plasmas are not uniform, spatial gradients exist.

---

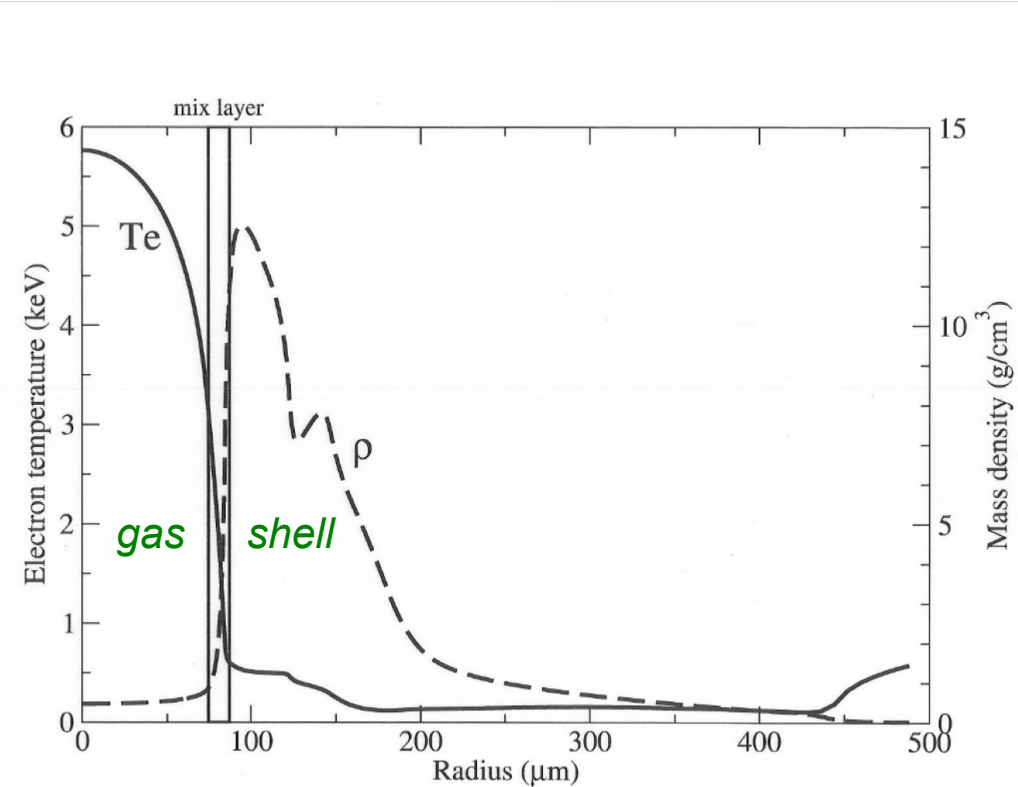


**Omega** shot 60897, XRFC4  
broadband image reconstructed  
from the MMI using the IDL tool by  
Taisuke Nagayama (UNR/Sandia)

# Plasmas are not uniform, spatial gradients exist.



**Omega shot** 60897, XRFC4  
broadband image reconstructed  
from the MMI using the IDL tool by  
Taisuke Nagayama (UNR/Sandia)



**NIF shot** N130617  
modeled with RAGE  
by Paul Bradley (XCP-6)

# Spectral modeling needs to account for:

---

- Photon emission
- Radiation

# Spectral modeling needs to account for:

---

- Opacity
  - Photon emission
- Transfer of  
Radiation

# Spectral modeling needs to account for:

---

- Detailed lineshapes      Spectral
- Opacity                      Transfer of
- Photon emission              Radiation

# Spectral modeling needs to account for:

---

- Spatial gradients

Finite-



Element

- Detailed lineshapes

Spectral

- Opacity

Transfer of

- Photon emission

Radiation

# Outline

---

- Motivation
- Implementation
- Examples
- Future work

# We are solving the radiation-transport equation

$$\frac{dI_\nu}{ds} = \varepsilon_\nu - \kappa_\nu I_\nu \rightarrow I_\nu = I_\nu^0 e^{-\kappa_\nu L} + \frac{\varepsilon_\nu}{\kappa_\nu} (1 - e^{-\kappa_\nu L})$$

*transmission  
of external  
radiation  $I_\nu^0$*       *self-emission  
including the effect  
of self-absorption*

- steady-state ( $c \rightarrow \infty$ )
- along a ray (3-D broken into 1-D pieces)      Solution for a uniform material is analytic.
- no scattering contribution to emission

$I_\nu$  : specific intensity (  $W \cdot cm^{-2} \cdot sr^{-1} \cdot eV^{-1}$  )

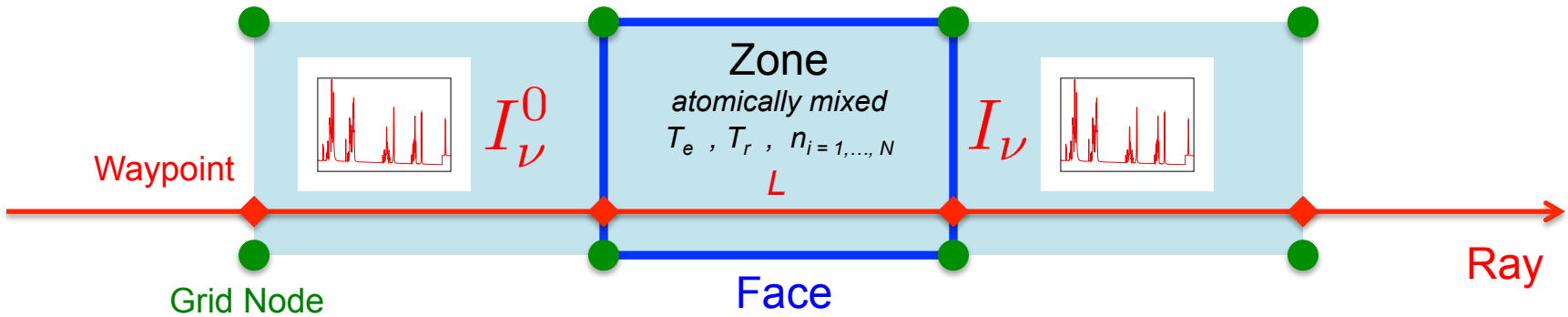
$\varepsilon_\nu$  : emissivity (  $W \cdot cm^{-3} \cdot sr^{-1} \cdot eV^{-1}$  )

$\kappa_\nu$  : opacity (  $cm^{-1}$  )

$L$  : chord length (  $cm$  )

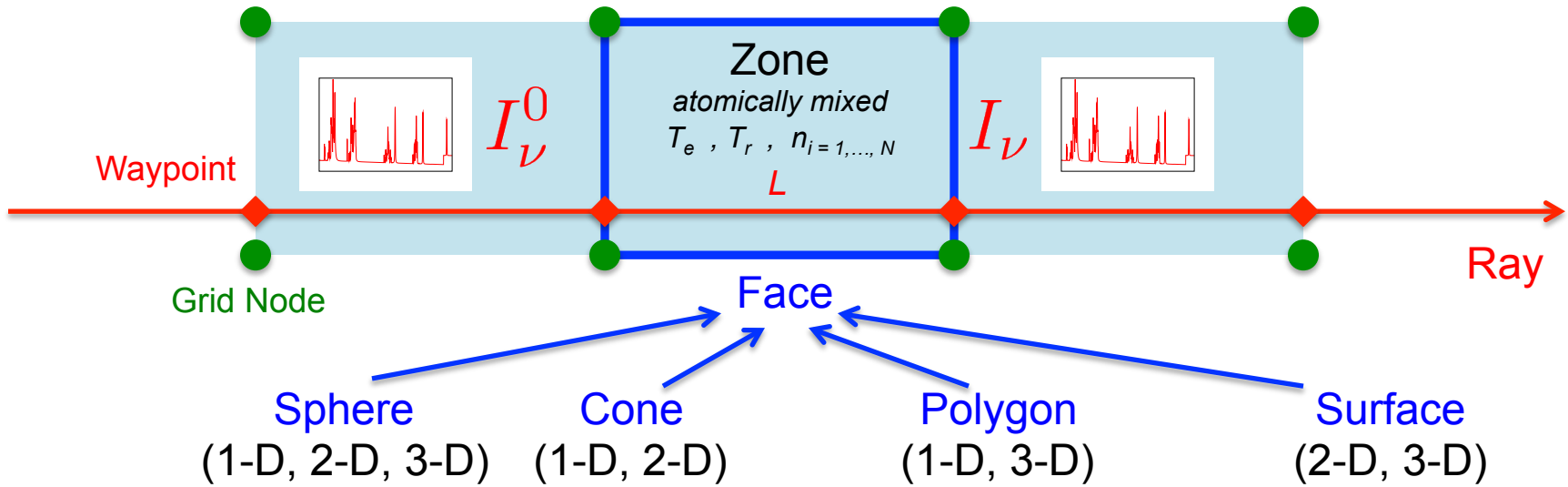
# Zones are the Finite Elements of FESTR

$$\frac{dI_\nu}{ds} = \varepsilon_\nu - \kappa_\nu I_\nu \rightarrow I_\nu = I_\nu^0 e^{-\kappa_\nu L} + \frac{\varepsilon_\nu}{\kappa_\nu} (1 - e^{-\kappa_\nu L})$$



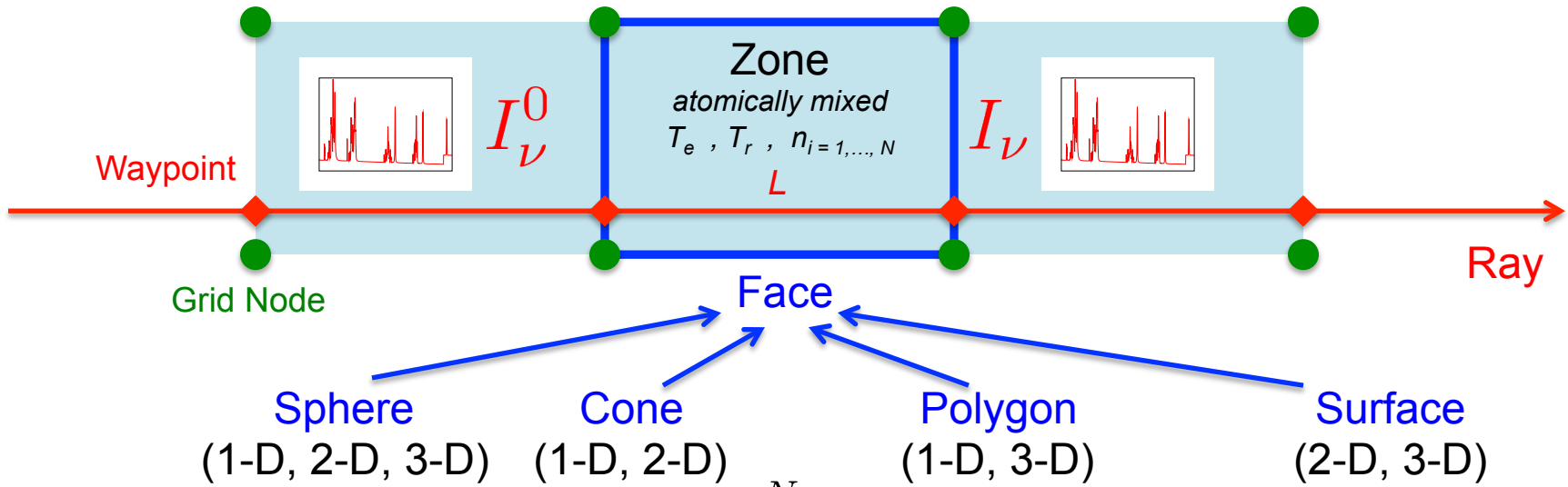
# Rays are traced across unstructured 3-D mesh

$$\frac{dI_\nu}{ds} = \varepsilon_\nu - \kappa_\nu I_\nu \rightarrow I_\nu = I_\nu^0 e^{-\kappa_\nu L} + \frac{\varepsilon_\nu}{\kappa_\nu} (1 - e^{-\kappa_\nu L})$$



# Mixed materials share a common electron density

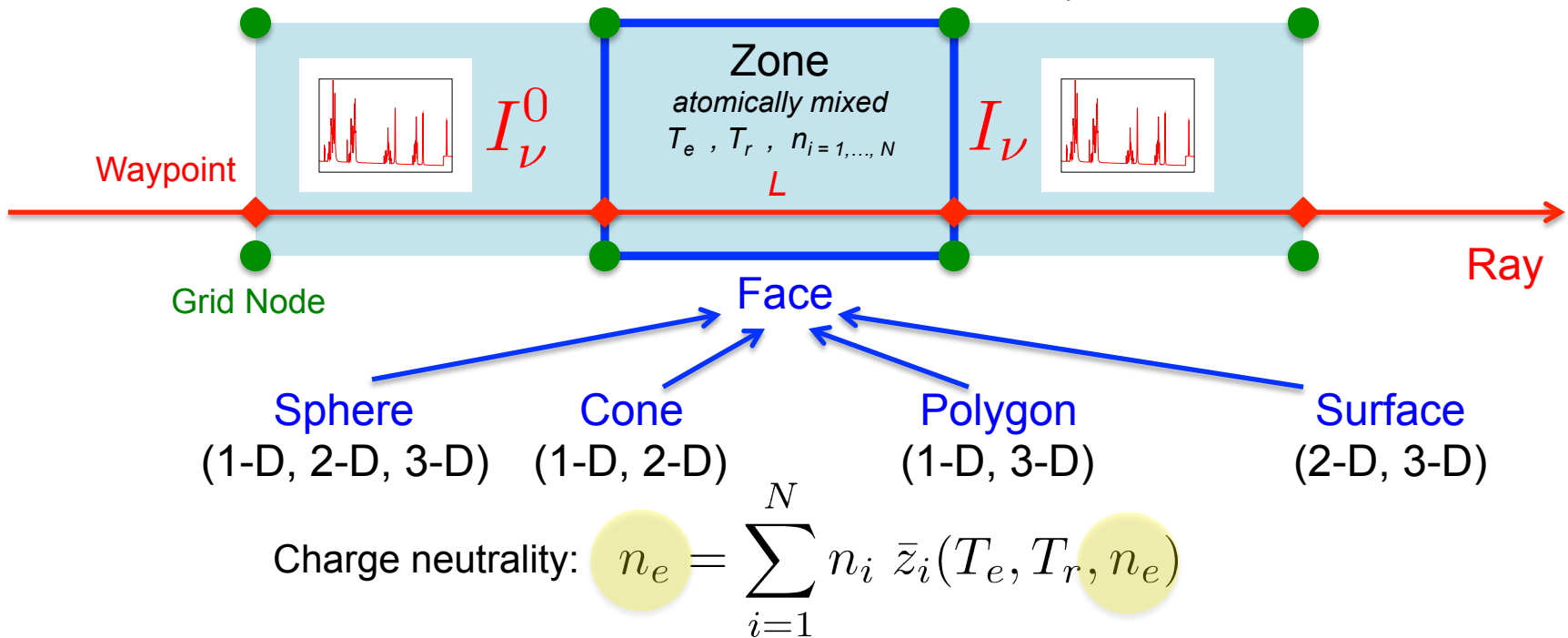
$$\frac{dI_\nu}{ds} = \varepsilon_\nu - \kappa_\nu I_\nu \rightarrow I_\nu = I_\nu^0 e^{-\kappa_\nu L} + \frac{\varepsilon_\nu}{\kappa_\nu} (1 - e^{-\kappa_\nu L})$$



$$\text{Charge neutrality: } n_e = \sum_{i=1}^N n_i \bar{z}_i(T_e, T_r, n_e)$$

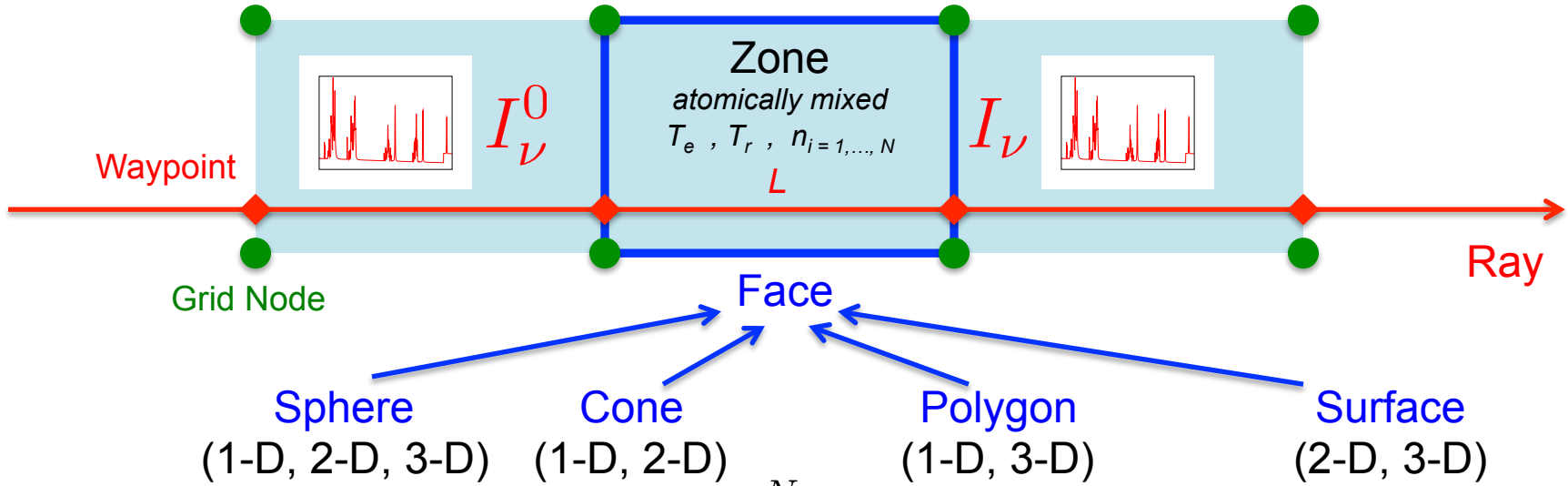
# TOPS-style search finds this common $n_e$

$$\frac{dI_\nu}{ds} = \varepsilon_\nu - \kappa_\nu I_\nu \rightarrow I_\nu = I_\nu^0 e^{-\kappa_\nu L} + \frac{\varepsilon_\nu}{\kappa_\nu} (1 - e^{-\kappa_\nu L})$$



# Atomic mixing of optical properties

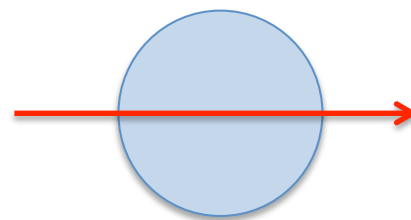
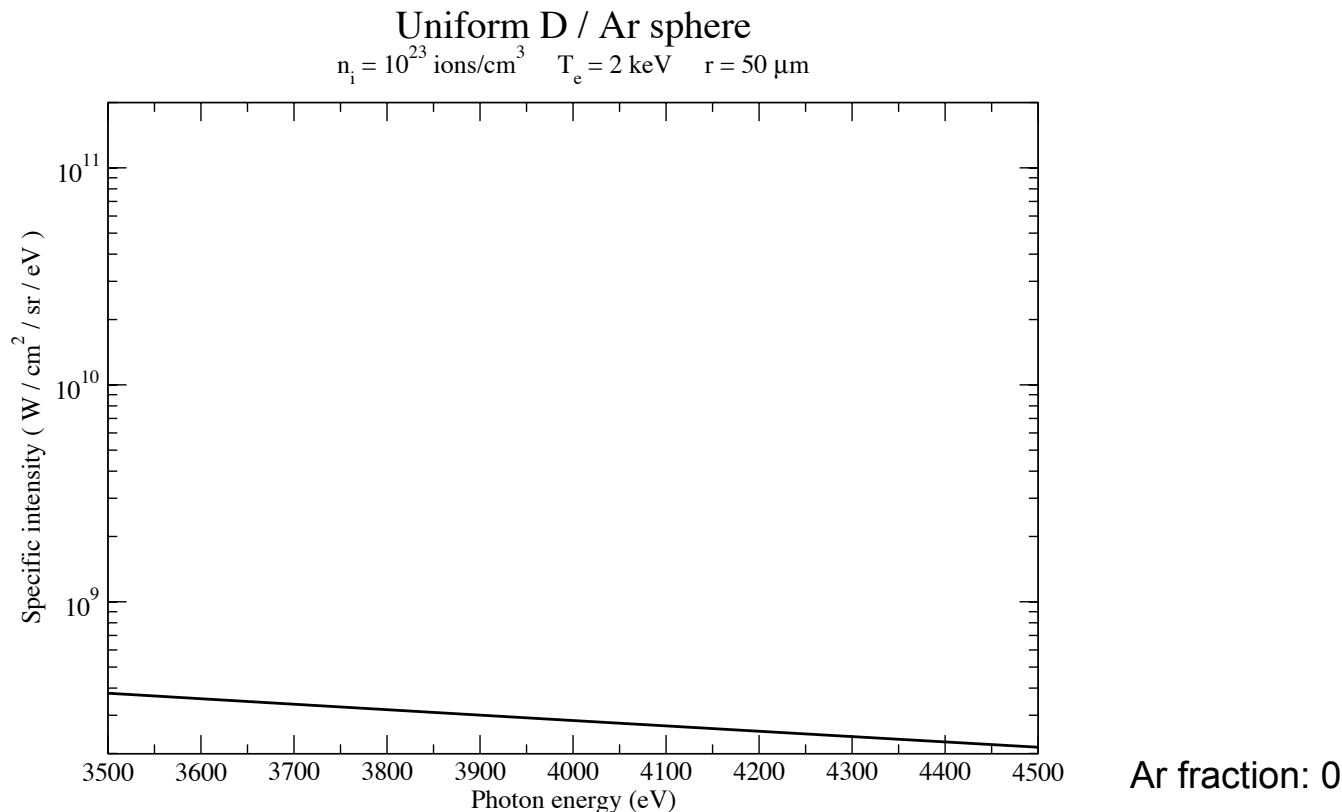
$$\frac{dI_\nu}{ds} = \varepsilon_\nu - \kappa_\nu I_\nu \rightarrow I_\nu = I_\nu^0 e^{-\kappa_\nu L} + \frac{\varepsilon_\nu}{\kappa_\nu} (1 - e^{-\kappa_\nu L})$$



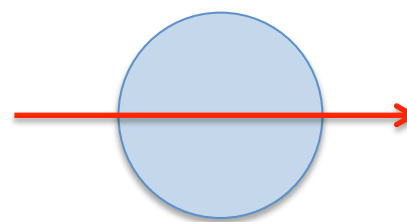
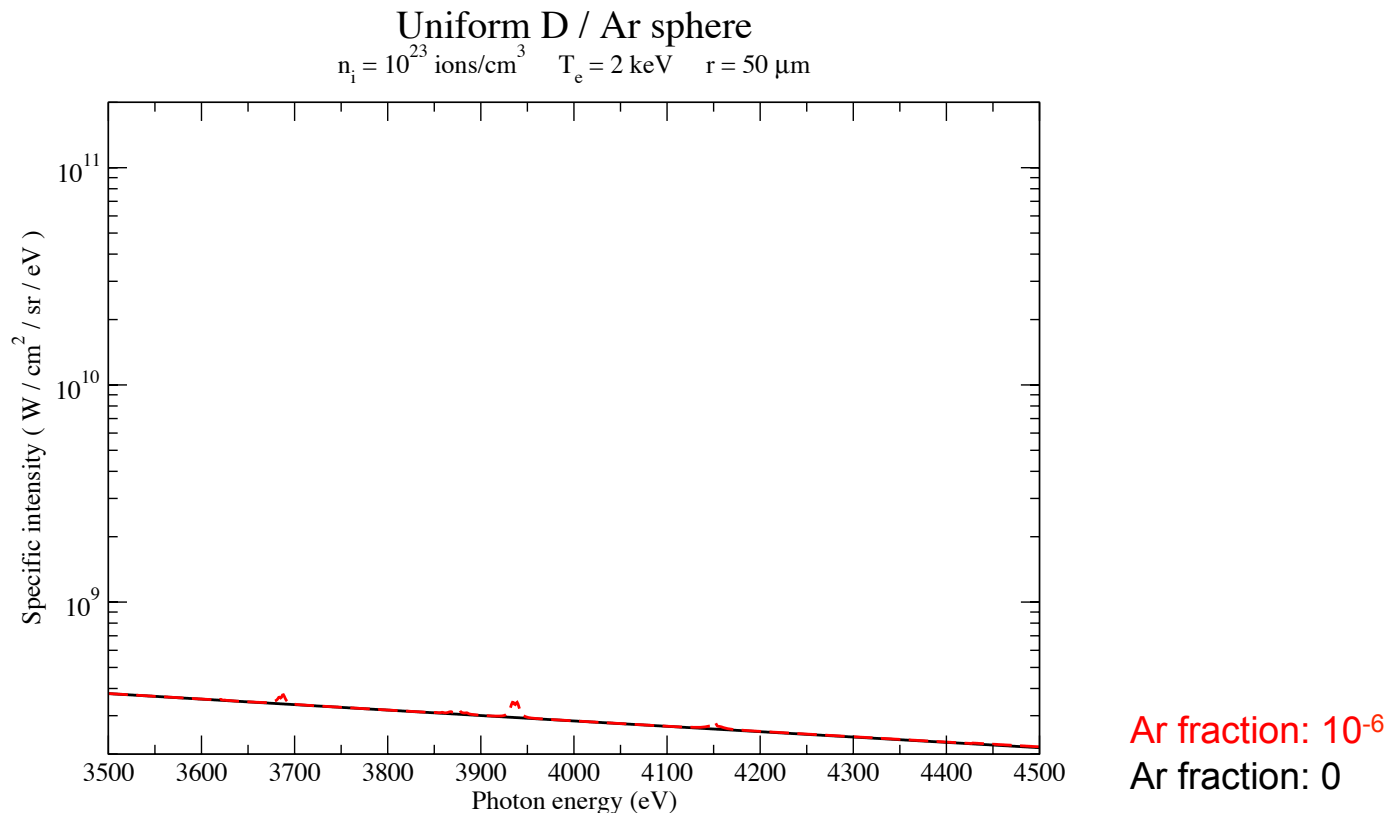
Charge neutrality:  $n_e = \sum_{i=1}^N n_i \bar{z}_i(T_e, T_r, n_e)$

Mixed emissivity:  $\varepsilon_\nu = \sum_{i=1}^N n_i \varepsilon_{i\nu}^A(T_e, T_r, n_e)$

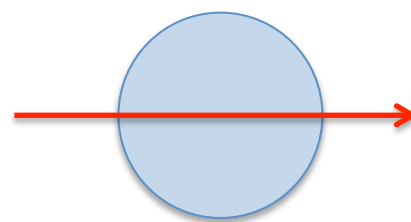
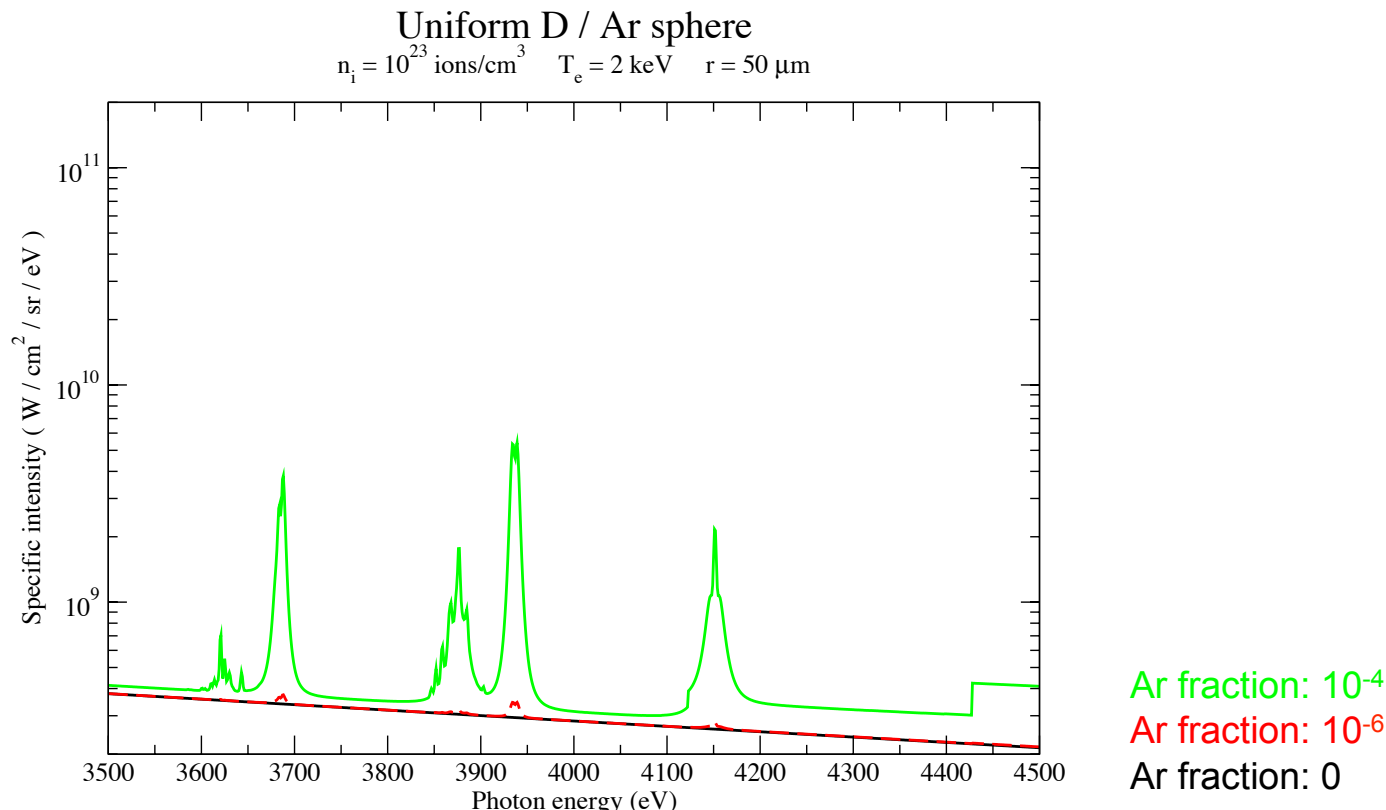
# Example of a mixed material calculation



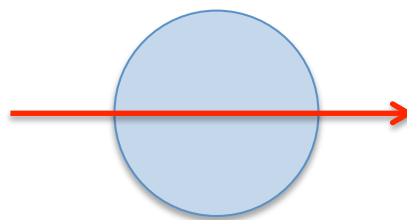
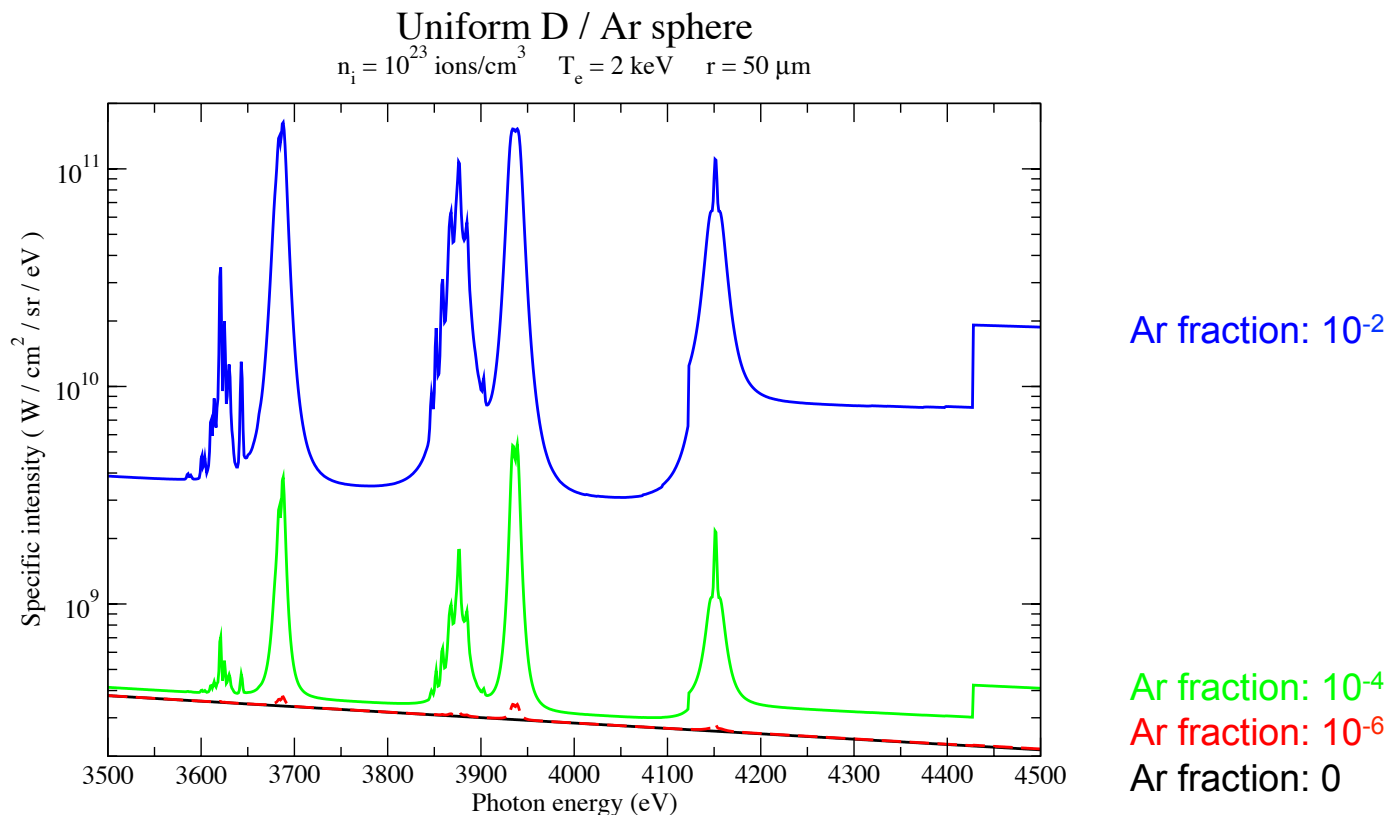
# Example of a mixed material calculation



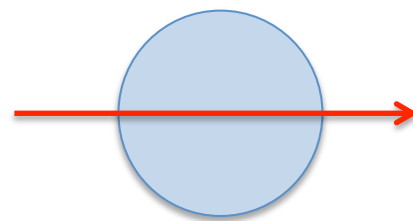
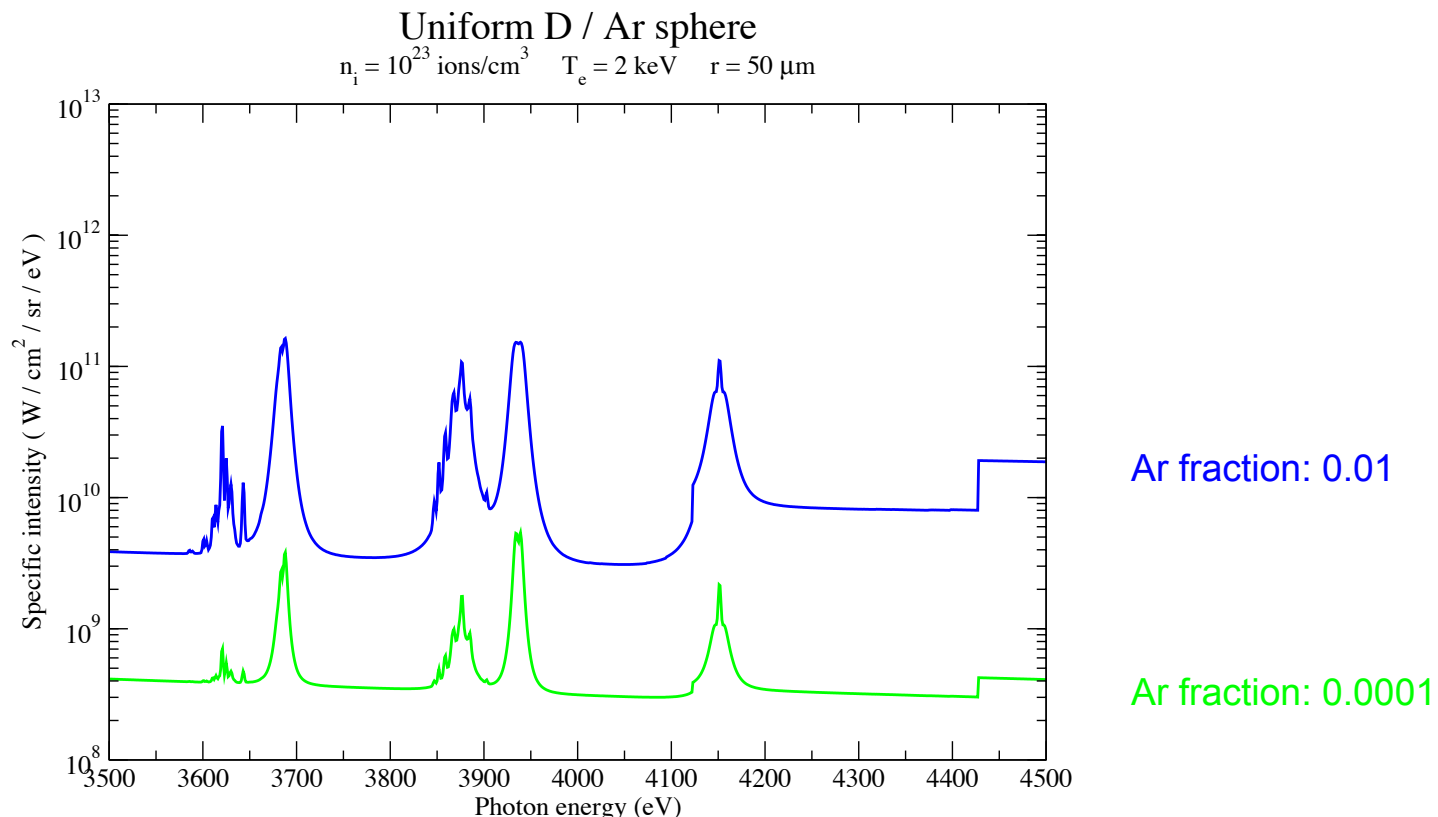
# Example of a mixed material calculation



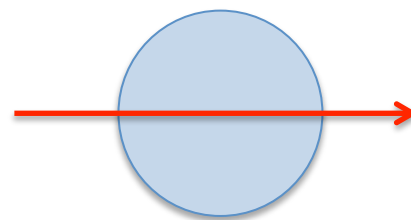
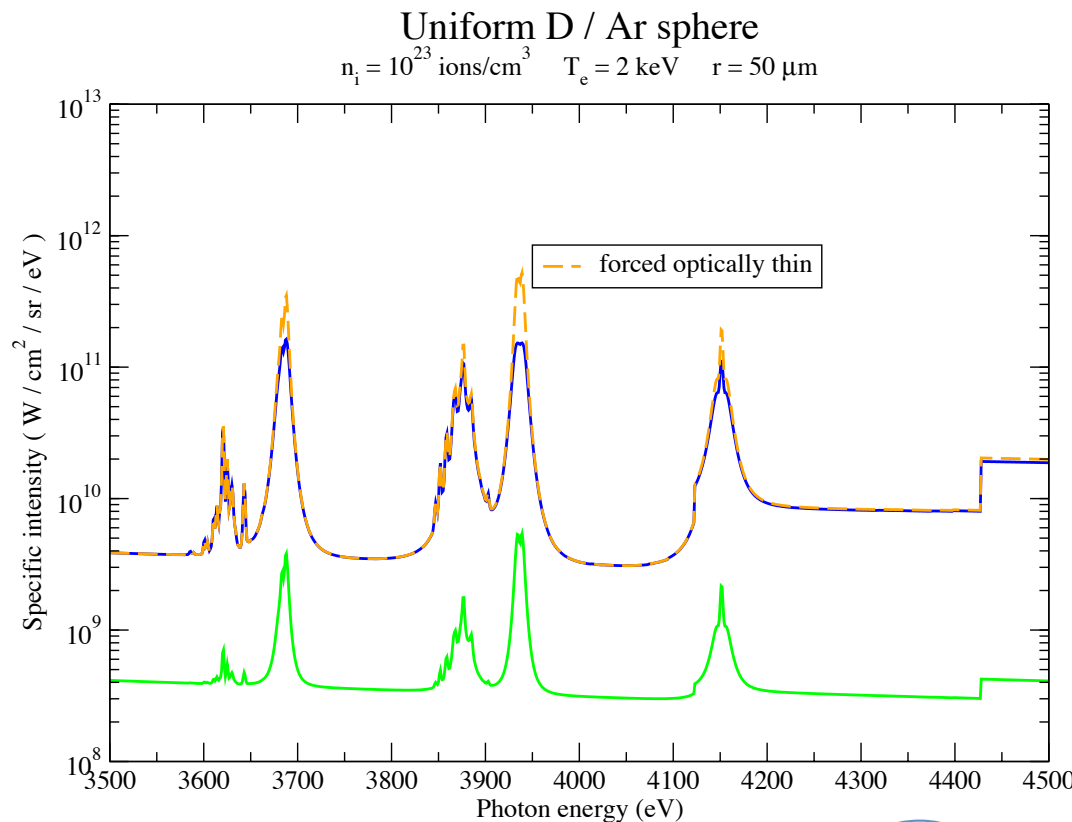
# Example of a mixed material calculation



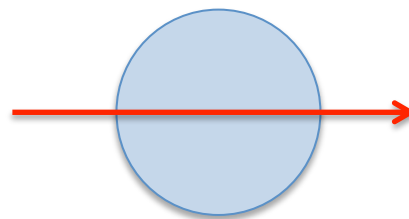
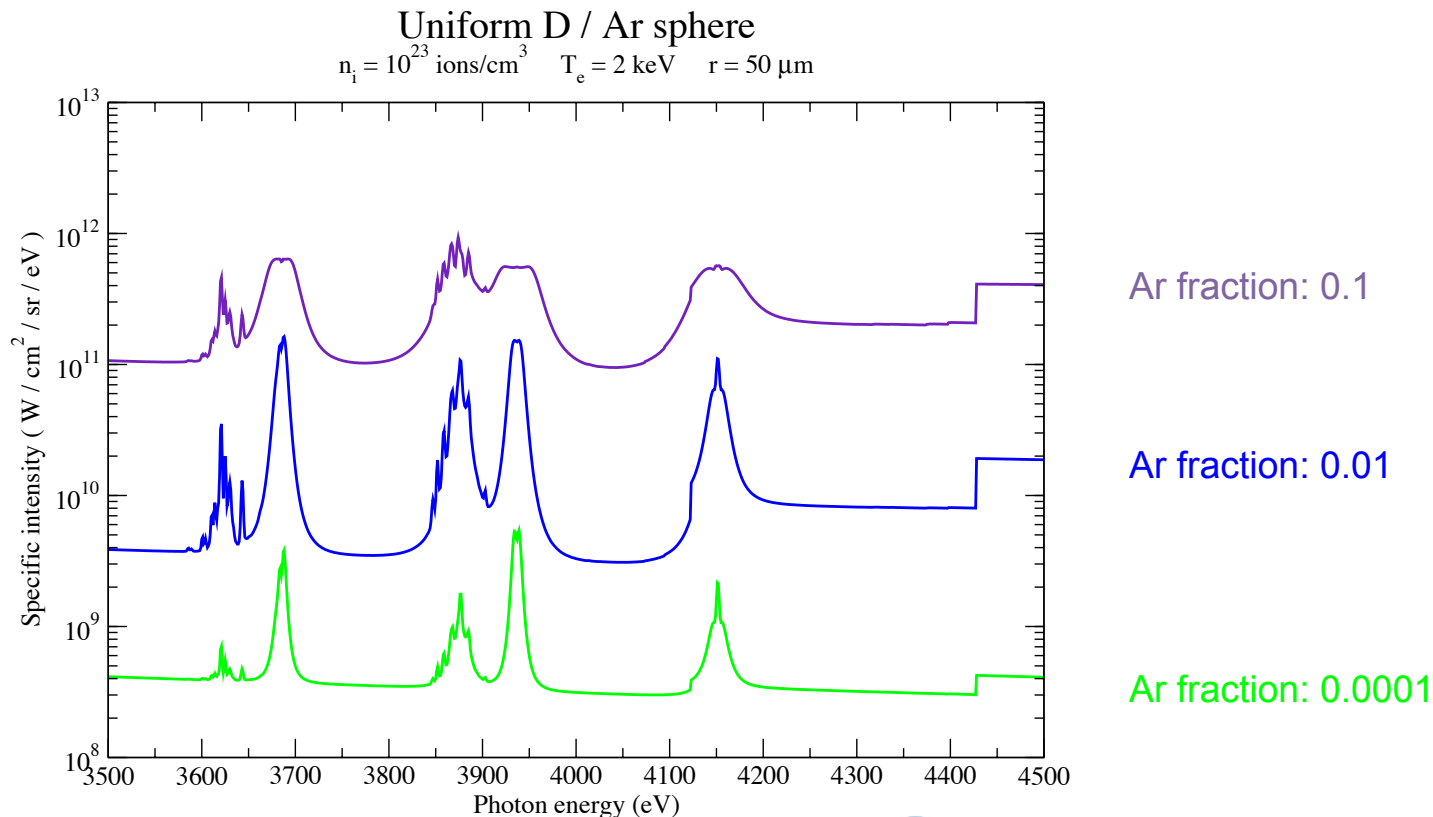
# Example of a mixed material calculation



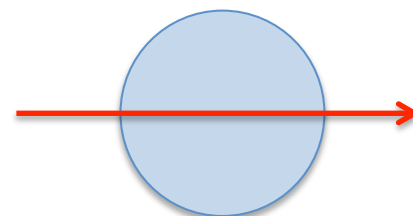
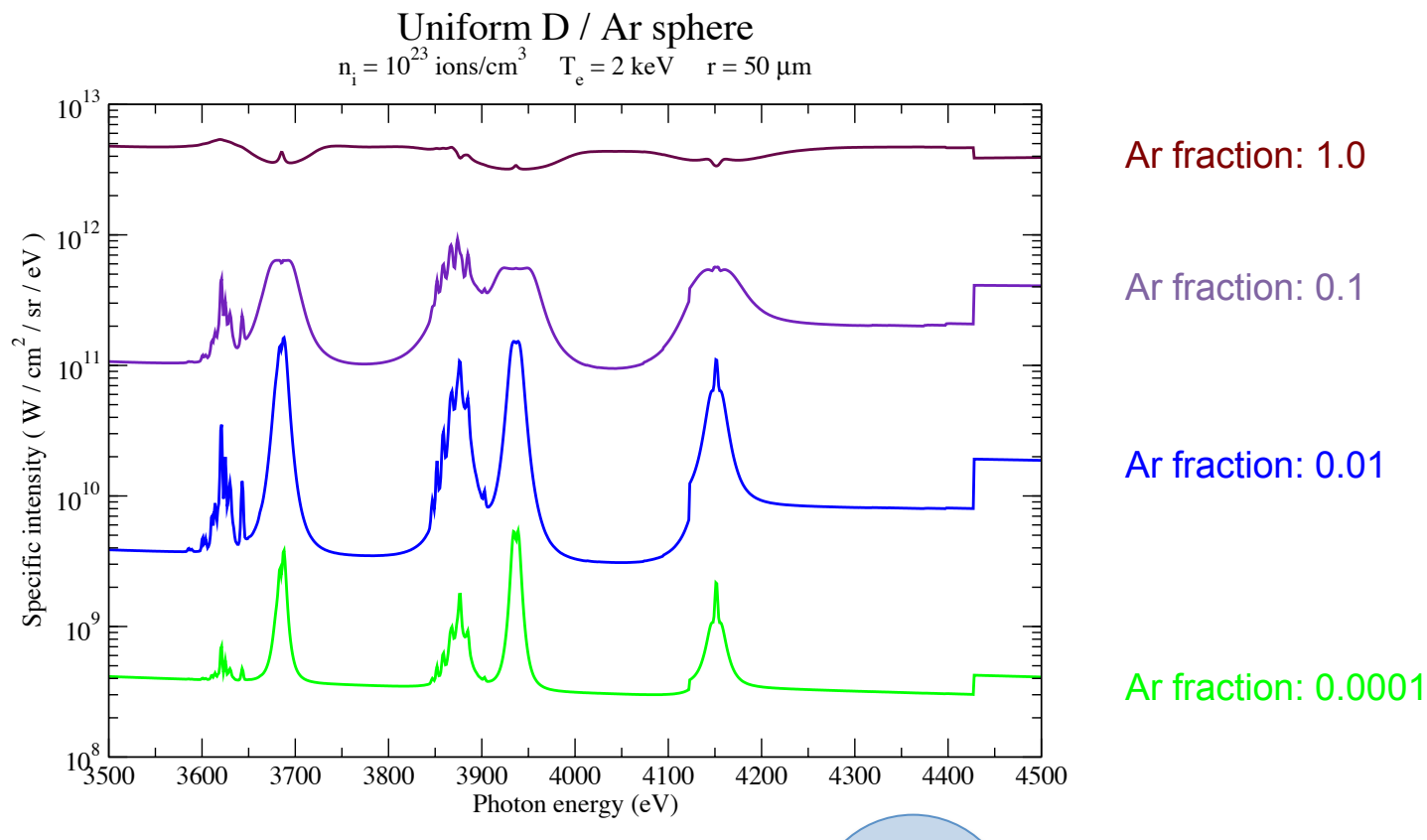
# Example of a mixed material calculation



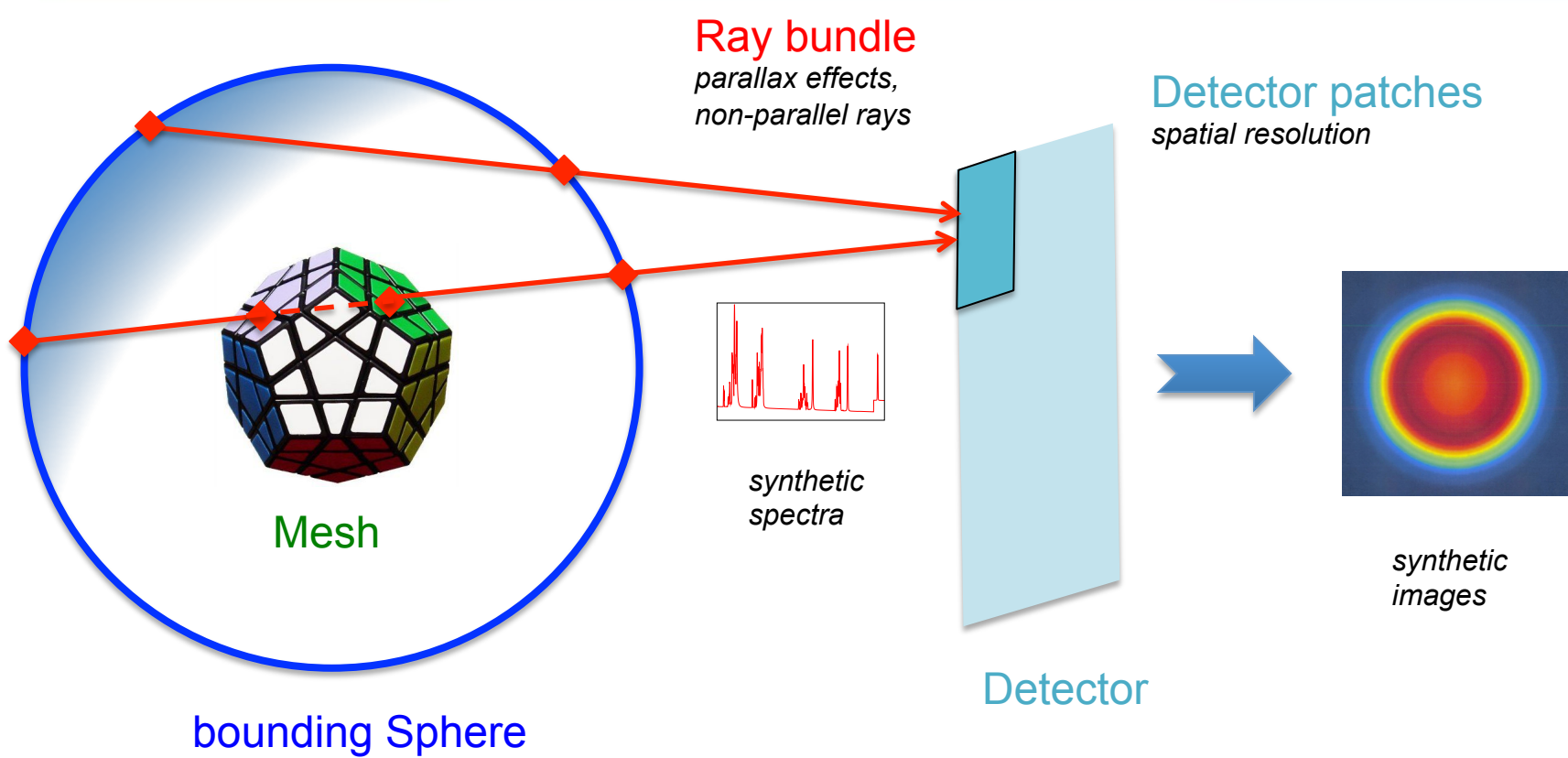
# Example of a mixed material calculation



# Example of a mixed material calculation

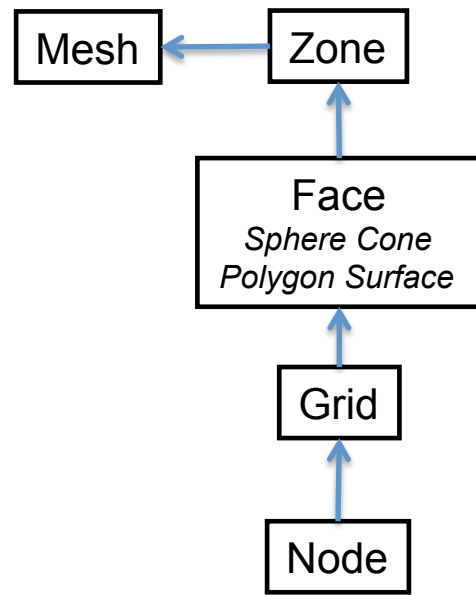


# Raytracing and diagnostics



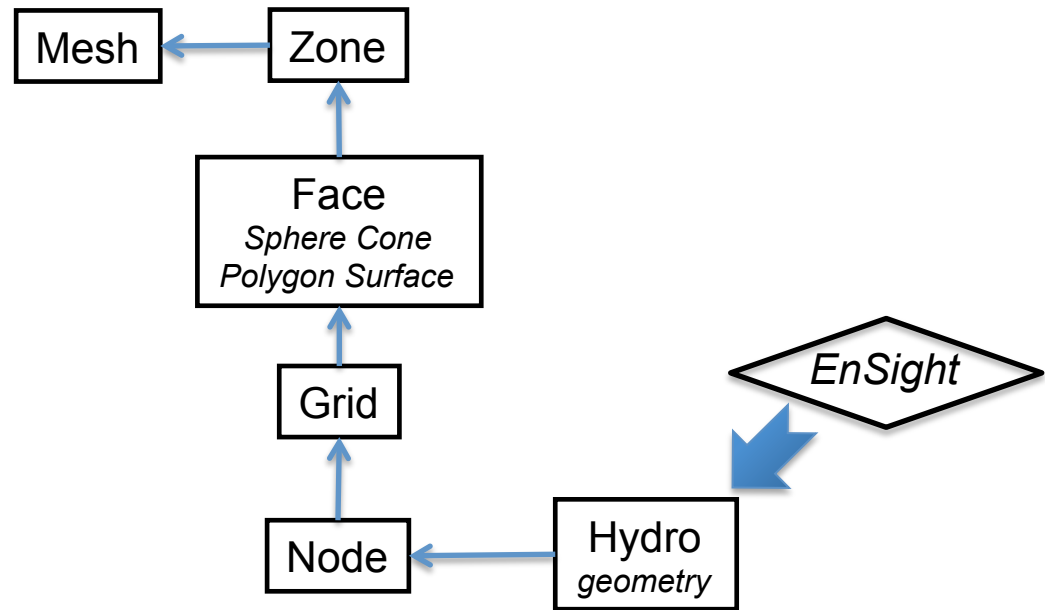
# FESTR class chart

---

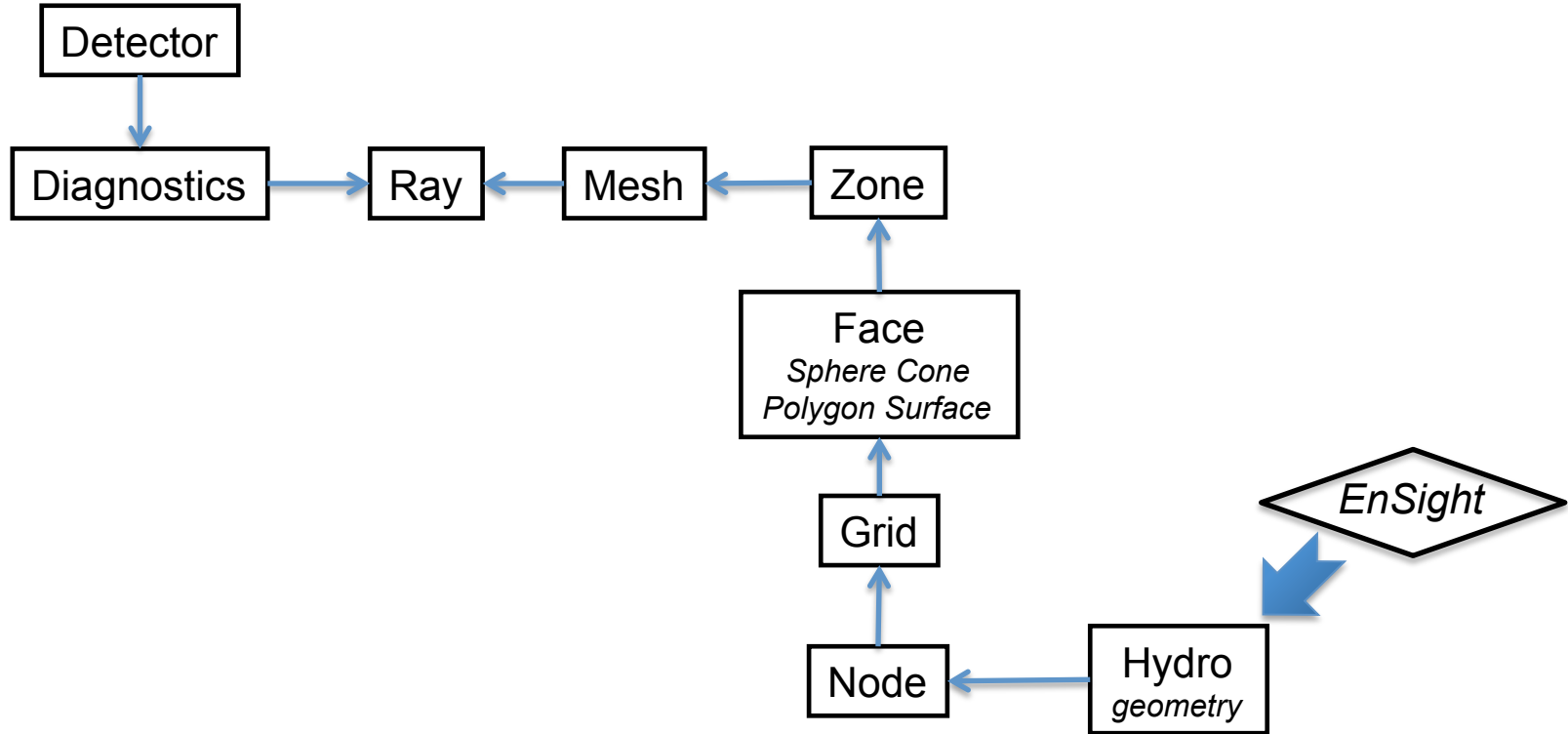


# FESTR class chart

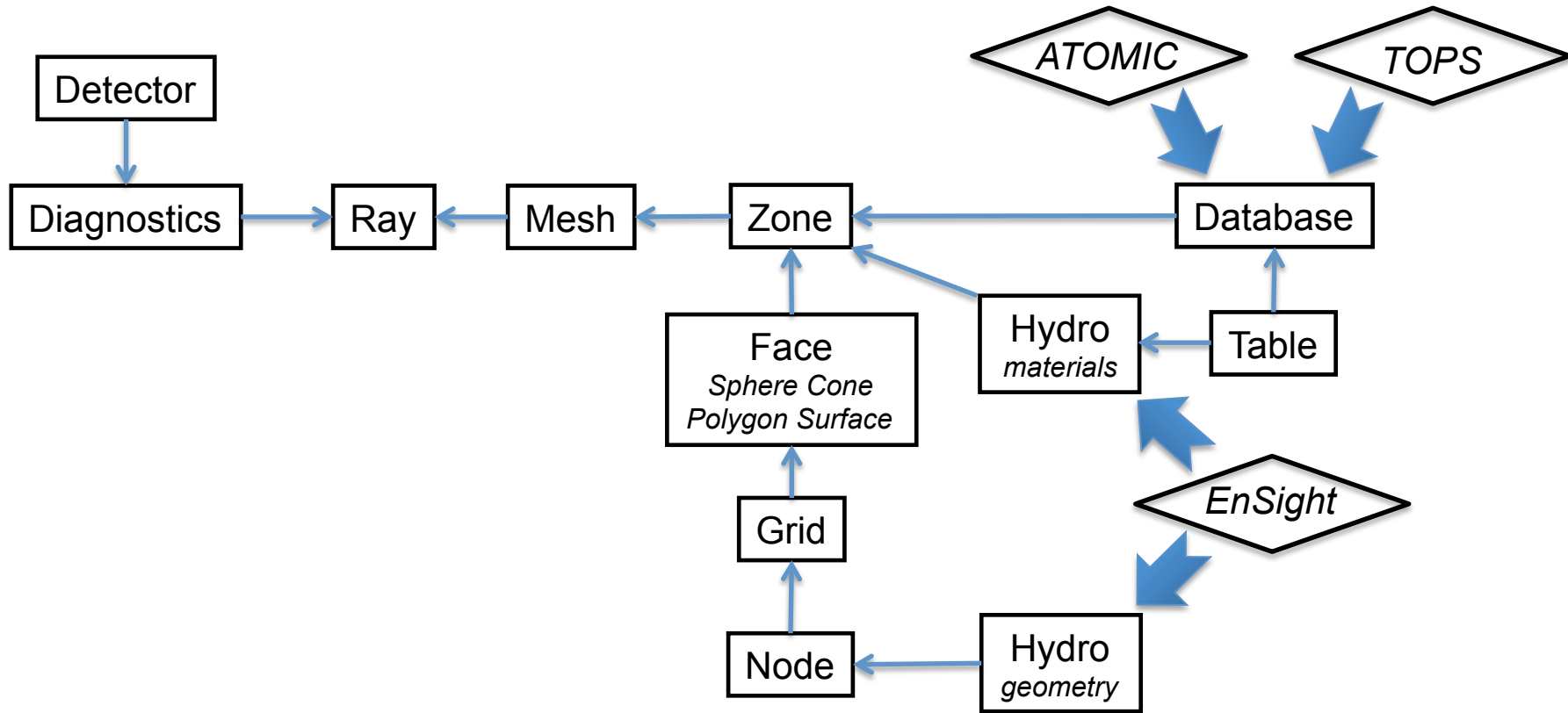
---



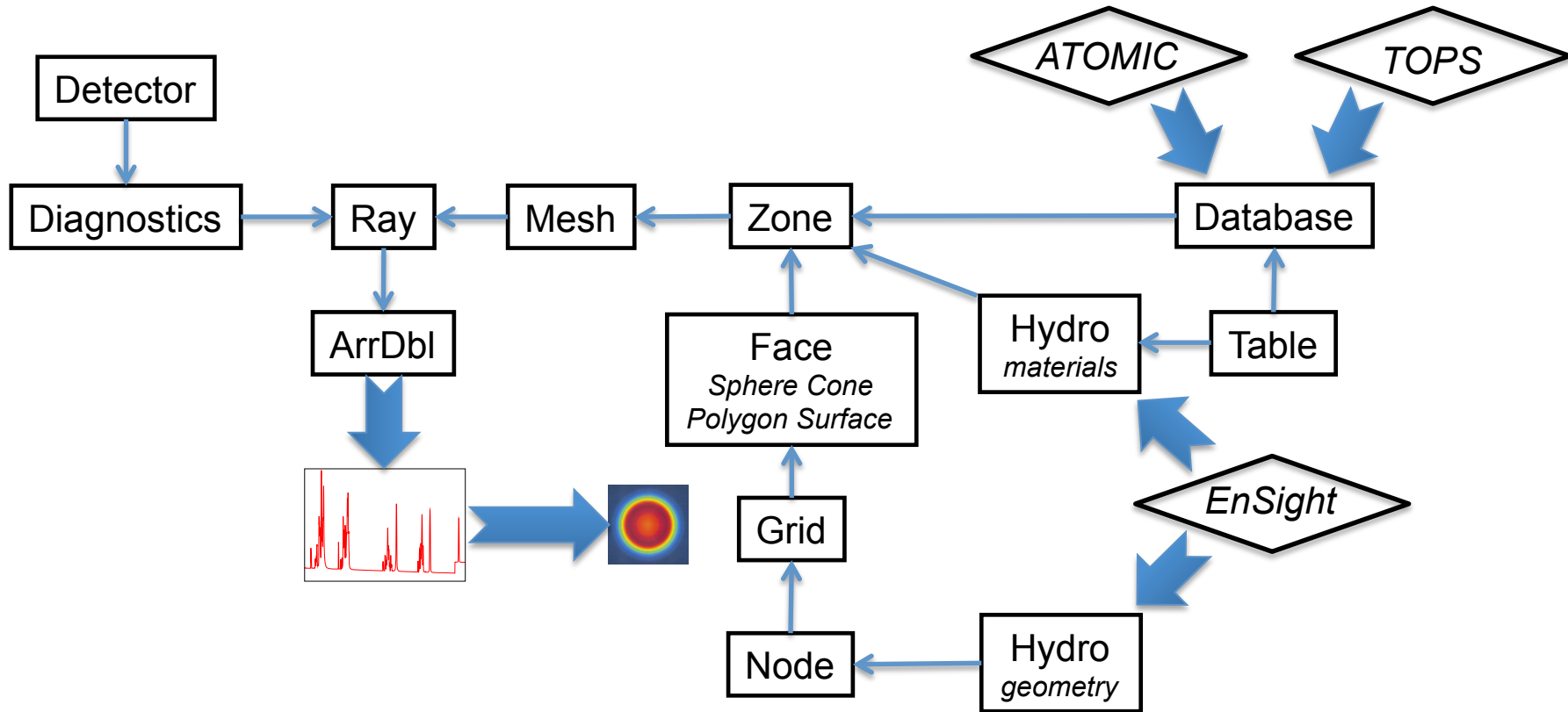
# FESTR class chart



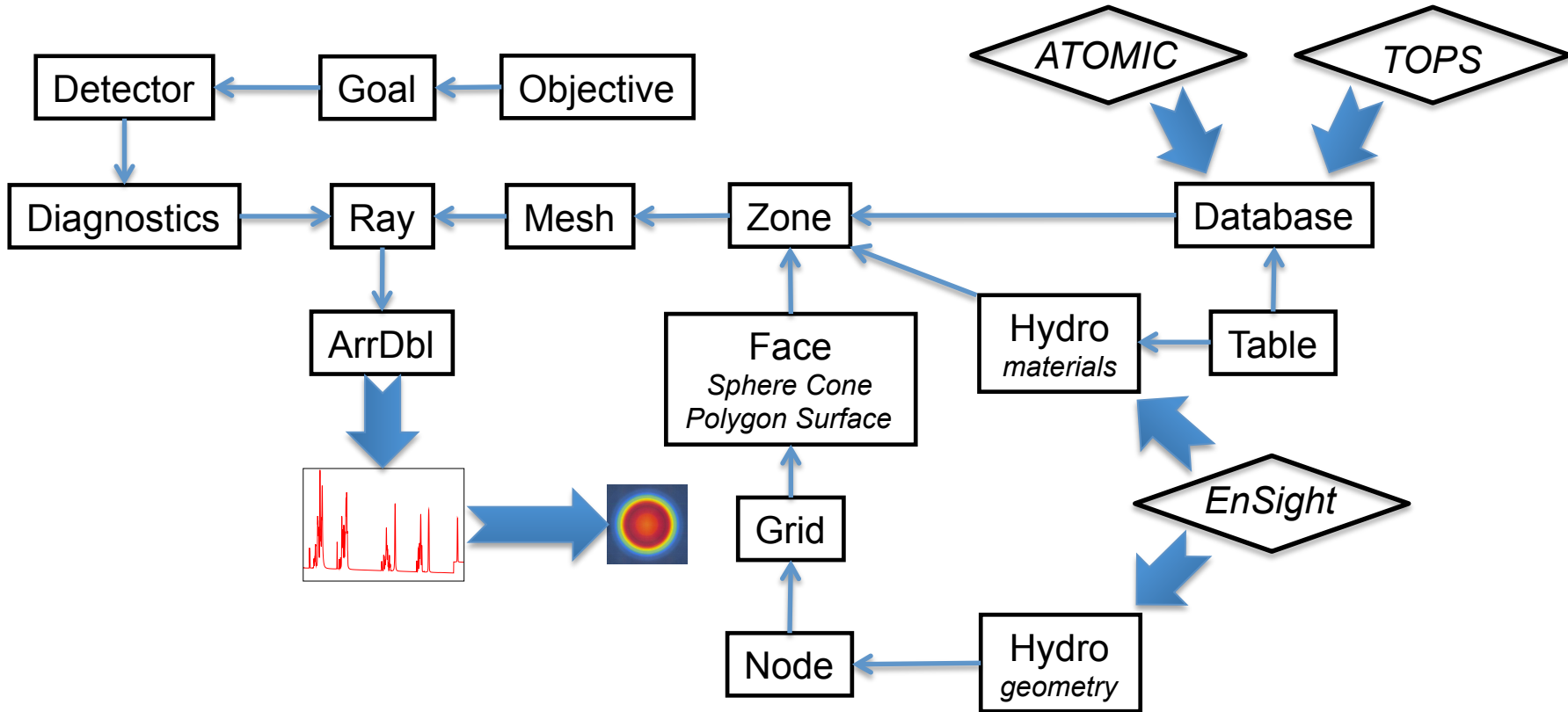
# FESTR class chart



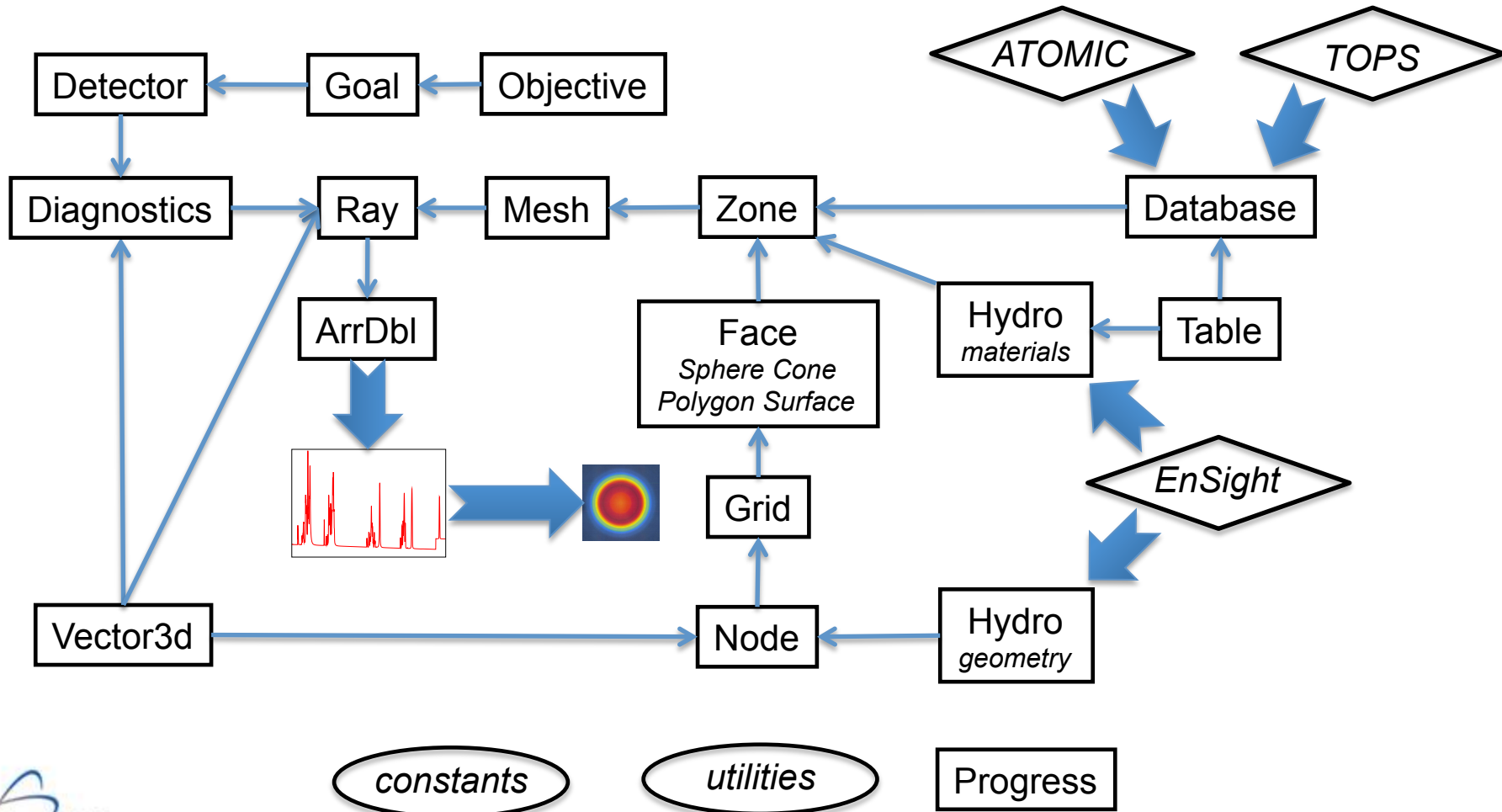
# FESTR class chart



# FESTR class chart



# FESTR class chart



# Design features

---

- **Modularity and reusability of components**
  - large number of short routines and small files
- **Design by contract**
  - specification of interfaces, up-to-date documentation
- **Test-driven development with unit tests**
  - simple, but general, native unit-test framework
- **Portability across platforms and compilers**
  - tested with Linux & Mac platforms, GNU / Intel / Portland compilers
- **Stateless kernels to aid future parallelization & threading**
  - data external to a class are passed via explicit argument lists instead of being shared via global variables

# Outline

---

- Motivation
- Implementation
- Examples
- Future work

# X-ray spectroscopic diagnostics and modeling of polar-drive implosion experiments on the National Ignition Facility

P. Hakel,<sup>1,a)</sup> G. A. Kyrala,<sup>1</sup> P. A. Bradley,<sup>1</sup> N. S. Krasheninnikova,<sup>1</sup> T. J. Murphy,<sup>1</sup> M. J. Schmitt,<sup>1</sup> I. L. Tregillis,<sup>1</sup> R. J. Kanzleiter,<sup>1</sup> S. H. Batha,<sup>1</sup> C. J. Fontes,<sup>1</sup> M. E. Sherrill,<sup>1</sup> D. P. Kilcrease,<sup>1</sup> and S. P. Regan<sup>2</sup>

<sup>1</sup>*Los Alamos National Laboratory, Los Alamos, New Mexico 87545, USA*

<sup>2</sup>*Laboratory for Laser Energetics, University of Rochester, Rochester, New York 14623-1299, USA*

(Received 26 March 2014; accepted 2 June 2014; published online 17 June 2014)

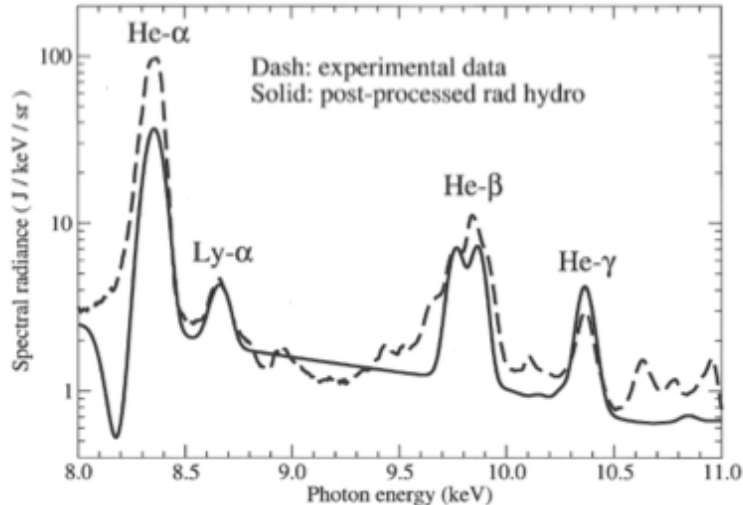


FIG. 9. Comparison of instrumentally broadened synthetic spectrum from post-processed rad hydro simulation with Supersnout II experimental data for the N130617 target (Cu dopant).

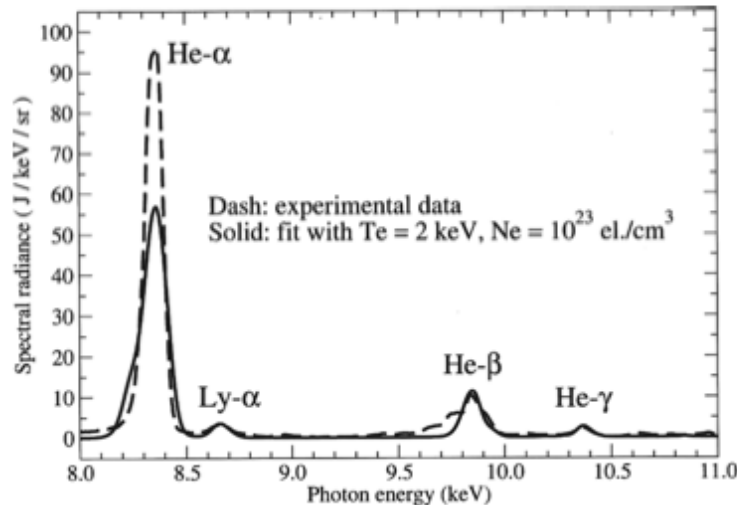


FIG. 11. Comparison of instrumentally broadened synthetic spectrum from a single temperature-density fit with continuum-subtracted Supersnout II experimental data for the N130617 target (Cu dopant).

# Observation of early shell-dopant mix in OMEGA direct-drive implosions and comparisons with radiation-hydrodynamic simulations

J. A. Baumgaertel,<sup>1</sup> P. A. Bradley,<sup>1</sup> S. C. Hsu,<sup>1</sup> J. A. Cobble,<sup>1</sup> P. Hakel,<sup>1</sup> I. L. Tregillis,<sup>1</sup> N. S. Krasheninnikova,<sup>1</sup> T. J. Murphy,<sup>1</sup> M. J. Schmitt,<sup>1</sup> R. C. Shah,<sup>1</sup> K. D. Obrey,<sup>1</sup> S. Batha,<sup>1</sup> H. Johns,<sup>2</sup> T. Joshi,<sup>2</sup> D. Mayes,<sup>2</sup> R. C. Mancini,<sup>2</sup> and T. Nagayama<sup>2,a)</sup>

<sup>1</sup>*Los Alamos National Laboratory, Los Alamos, New Mexico 87545, USA*

<sup>2</sup>*Physics Department, University of Nevada, Reno, Nevada 89557, USA*

(Received 12 February 2014; accepted 19 May 2014; published online 30 May 2014)

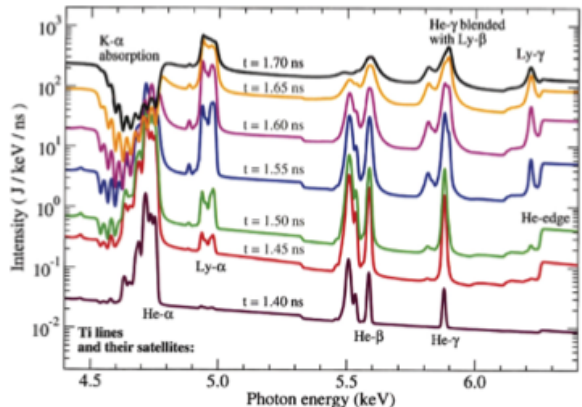


FIG. 7. The time dependence of the RAGE synthetic SSCA results for 65036, 50 nm mix run, qualitatively agrees with the experiment (Fig. 5). Lines are 50 ps apart, starting at 1.40 ns, in ascending order. The vertical shift is real and due to increasing emission as the capsule gets denser. These curves are computed on a photon-energy grid resolved to 1 eV and the displayed spectra include 11 eV of instrumental broadening of the SSCA instrument.<sup>43</sup>

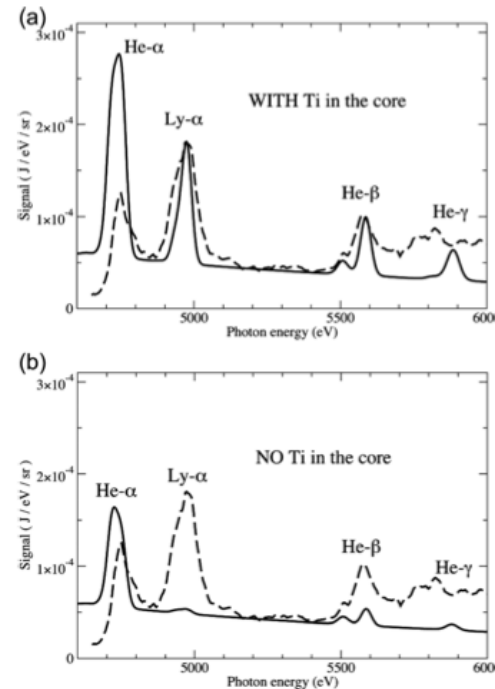
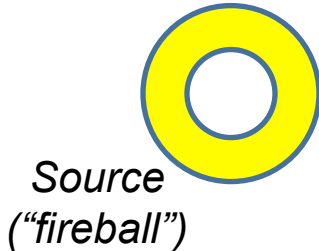


FIG. 10. The experimental MMI spectra (dashed line) is matched by ATOMIC (solid line) best when there is (a) 1.3 ng of Ti in the core, compared with (b), which has no Ti in the core.

# Application in visible / IR regime

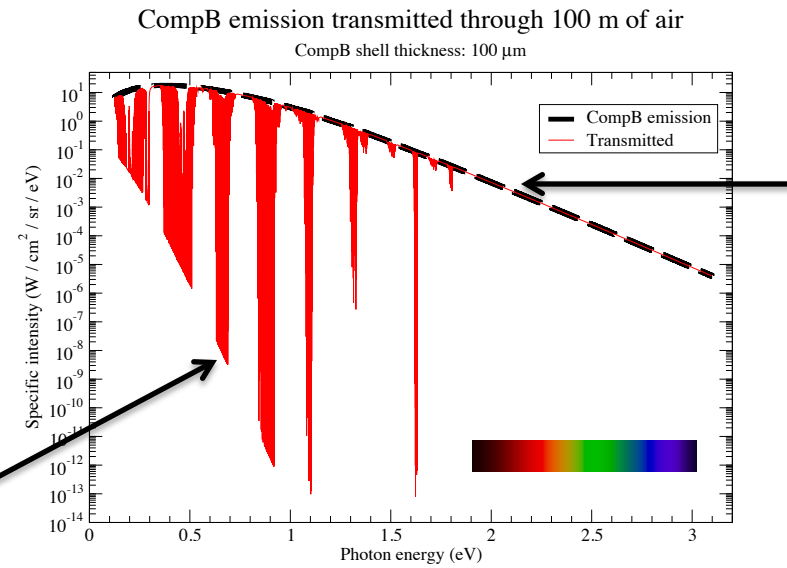
## CompB:

$T = 1574 \text{ K}$  (Planckian source)  
 $\rho = 0.5 \text{ g/cm}^3$   
thin shell, radius 15 cm  
spherical geometry



EOS and opacity data were provided by Eddy Timmermans (T-4), Josh Coe (T-1), Leanne Duffy (AOT-AE), Cristiano Nisoli (T-4), Dima Mozyrsky (T-4).

Spectrum no lower than the  $T = 296 \text{ K}$  Planckian (air)



Spectrum no higher than the  $T = 1574 \text{ K}$  Planckian (CompB)

Acknowledgements to Jim Reynolds (now at Sandia) Rod Whitaker (EES-17)



Contents lists available at ScienceDirect

## Spectrochimica Acta Part B

journal homepage: [www.elsevier.com/locate/sab](http://www.elsevier.com/locate/sab)

Letter to the Editor

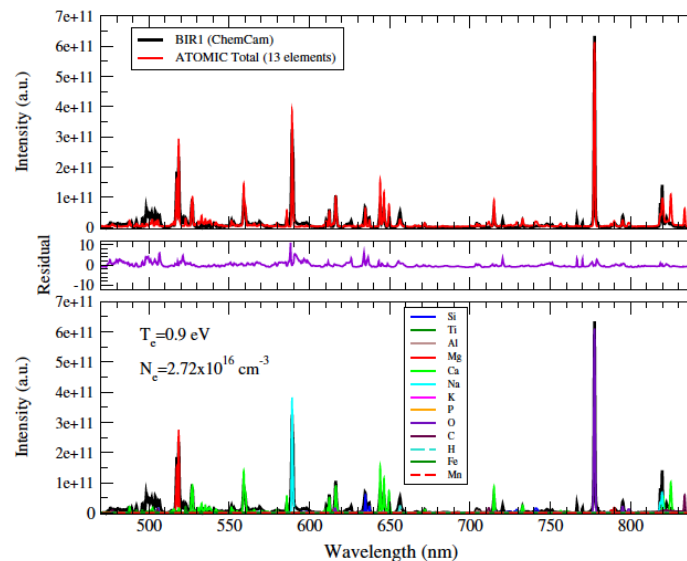
## Theoretical modeling and analysis of the emission spectra of a ChemCam standard: Basalt BIR-1A

J. Colgan <sup>a,\*</sup>, E.J. Judge <sup>b</sup>, H.M. Johns <sup>a</sup>, D.P. Kilcrease <sup>a</sup>, J.E. Barefield II <sup>b</sup>, R. McInroy <sup>c</sup>, P. Hakel <sup>d</sup>, R.C. Wiens <sup>e</sup>, S.M. Clegg <sup>c</sup>

24

J. Colgan et al. / Spectrochimica Acta Part B 110 (2015) 20–30

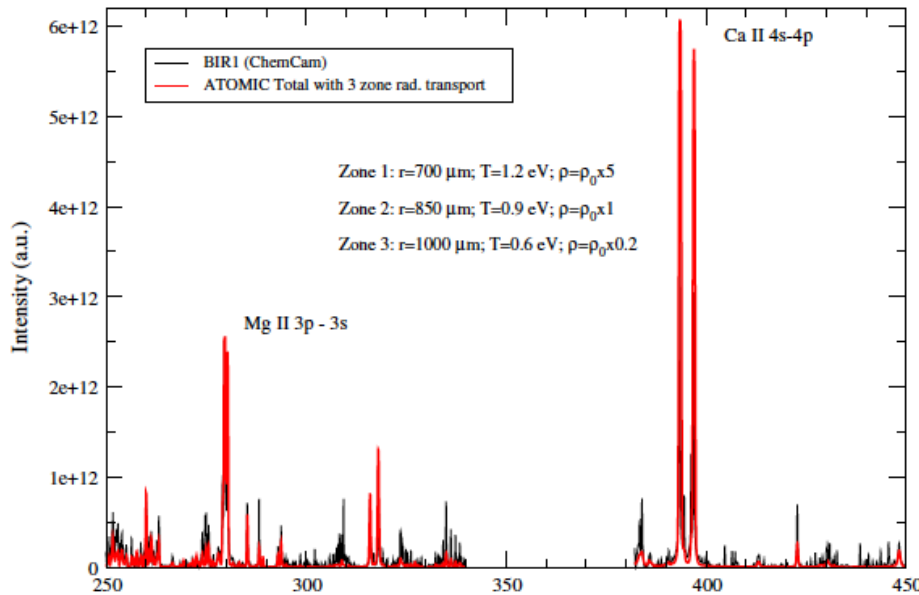
<sup>a</sup> Theoretical Division, Los Alamos National Laboratory  
<sup>b</sup> Chemical Diagnostics and Engineering, Los Alamos National Laboratory  
<sup>c</sup> Physical Chemistry and Applied Spectroscopy, Los Alamos National Laboratory  
<sup>d</sup> Computational Physics Division, Los Alamos National Laboratory  
<sup>e</sup> Space and Remote Sensing Division, Los Alamos National Laboratory



13 elements  
in the ATOMIC  
calculation!

visible / IR

Fig. 2. Comparison of the ChemCam spectra from the basalt sample BIR-1A with the ATOMIC multi-element LTE calculation at a temperature of 0.9 eV and for a wavelength range of 470 to 850 nm. The upper panel shows the total emissivity from ATOMIC (red line) versus the ChemCam basalt BIR-1A standard. The lower panel shows the contributions from the different elements present in the basalt plasma. The global electron density as computed from ATOMIC is also indicated. The middle panel shows a residual between the experimental data and the ATOMIC calculations as described in the text. (For interpretation of the references to color in this figure legend, the reader is referred to the web version of this article.)



near-visible / UV

Fig. 8. Emission spectrum of the Basalt sample in the near-visible region as computed from the ATOMIC calculations that include radiation transport through three plasma zones as described in the text. Each zone radius is indicated as well as the temperature in each zone. The densities used in each zone are factors of  $\rho_0$ , where  $\rho_0$  represents the mass densities of all the elements listed in Table 3.

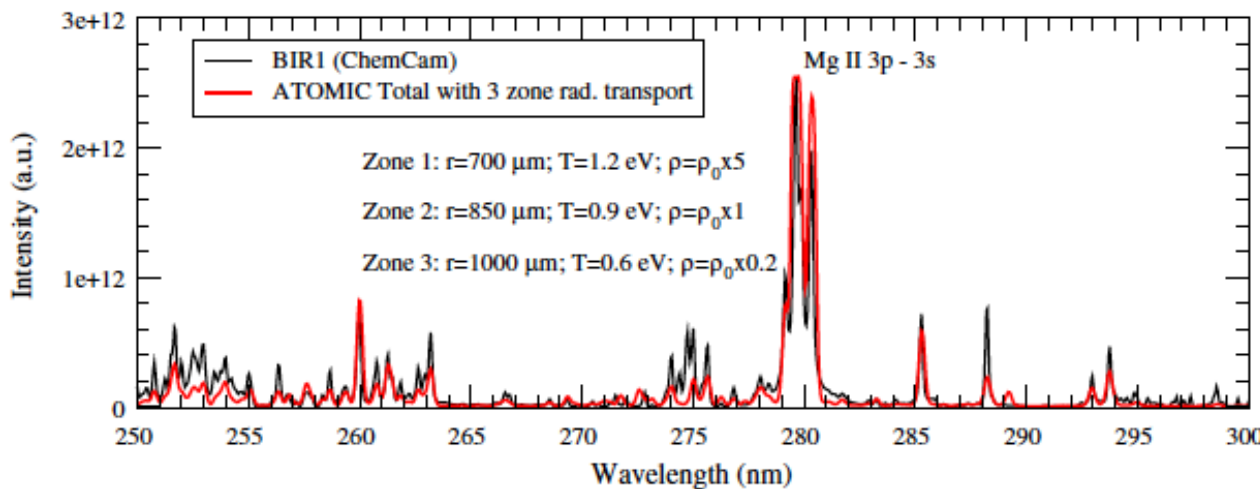
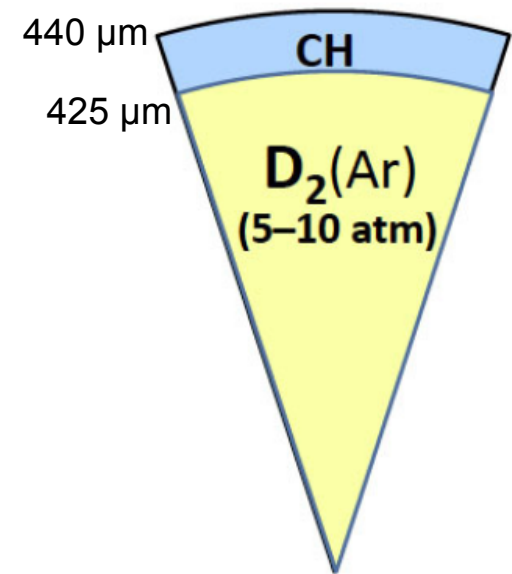


Fig. 9. Emission spectrum of the Basalt sample in the 250–300 nm region as computed from the ATOMIC calculations that include radiation transport through three plasma zones as described in the text.

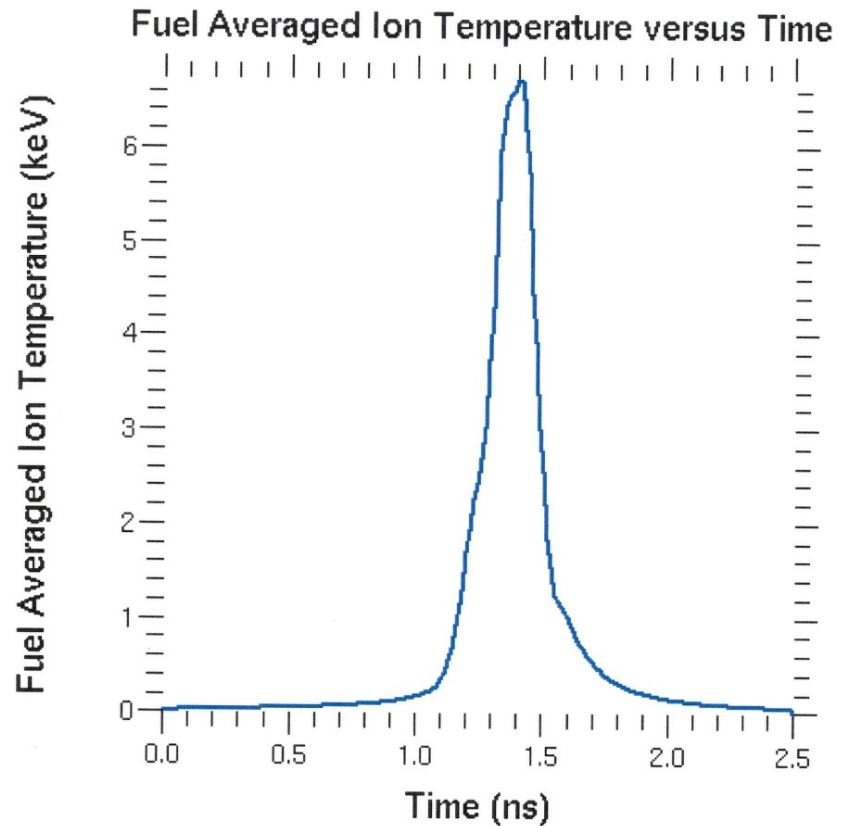
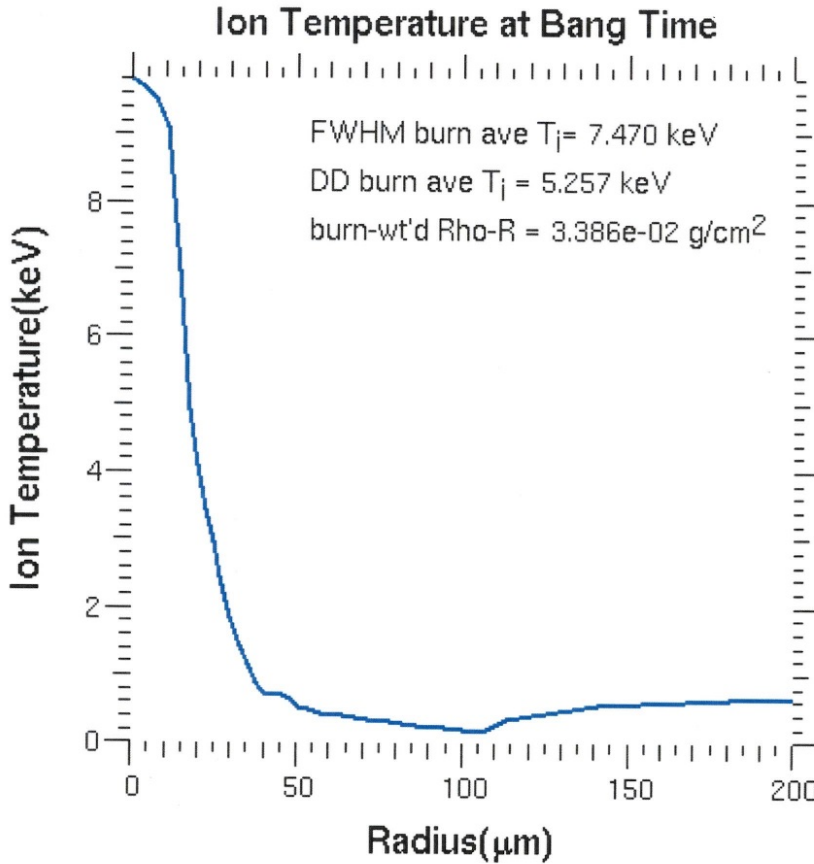
# KPE project: Hydra used to simulate OMEGA CH capsule with D<sub>2</sub> fill and 1% Ar dopant (5 atm total)

- 27 kJ, 1 ns, de-rated by 0.6
- 70-eV inner-shell preheat
- Shell should be thick enough (15  $\mu\text{m}$  here) not to burn through



Slide provided by Mark Schmitt (XCP-6)

# Ion temperature gets to >8 keV range as desired for strong interspecies diffusion

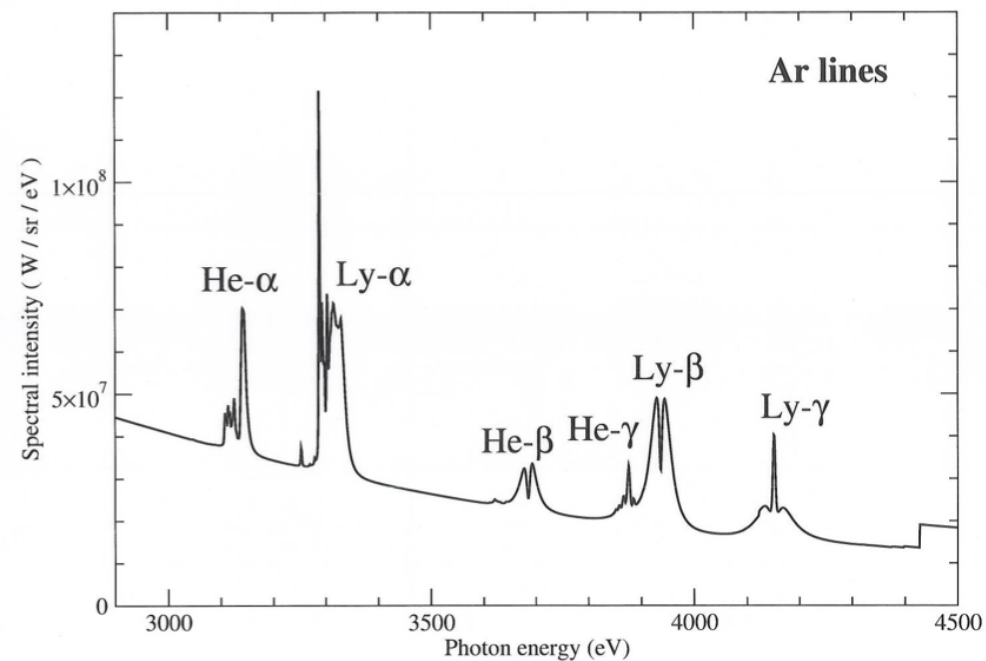


Slide provided by Mark Schmitt (XCP-6)

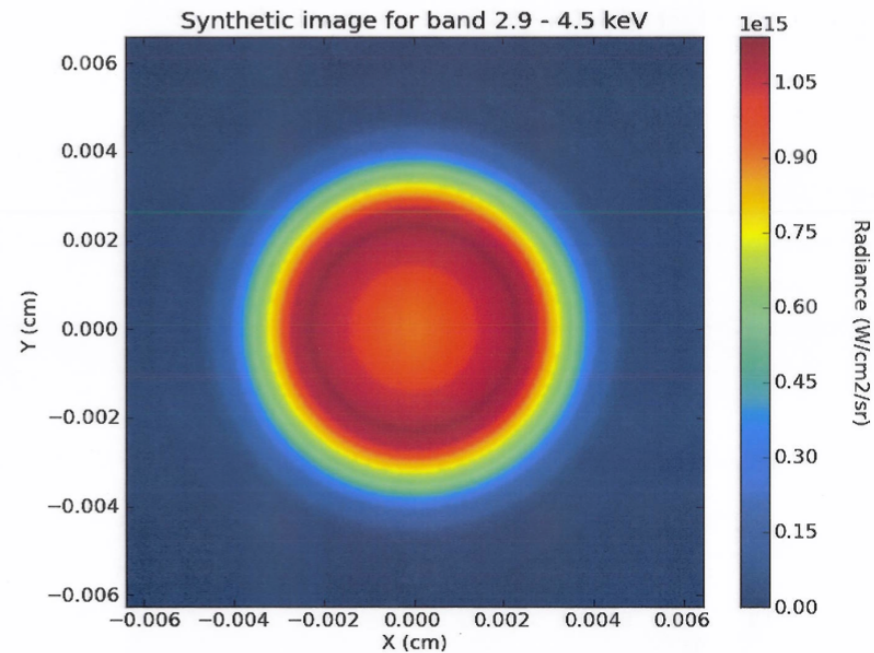
# Examples of a synthetic spectrum, image

Space-integrated instantaneous spectrum

April 6, 2015



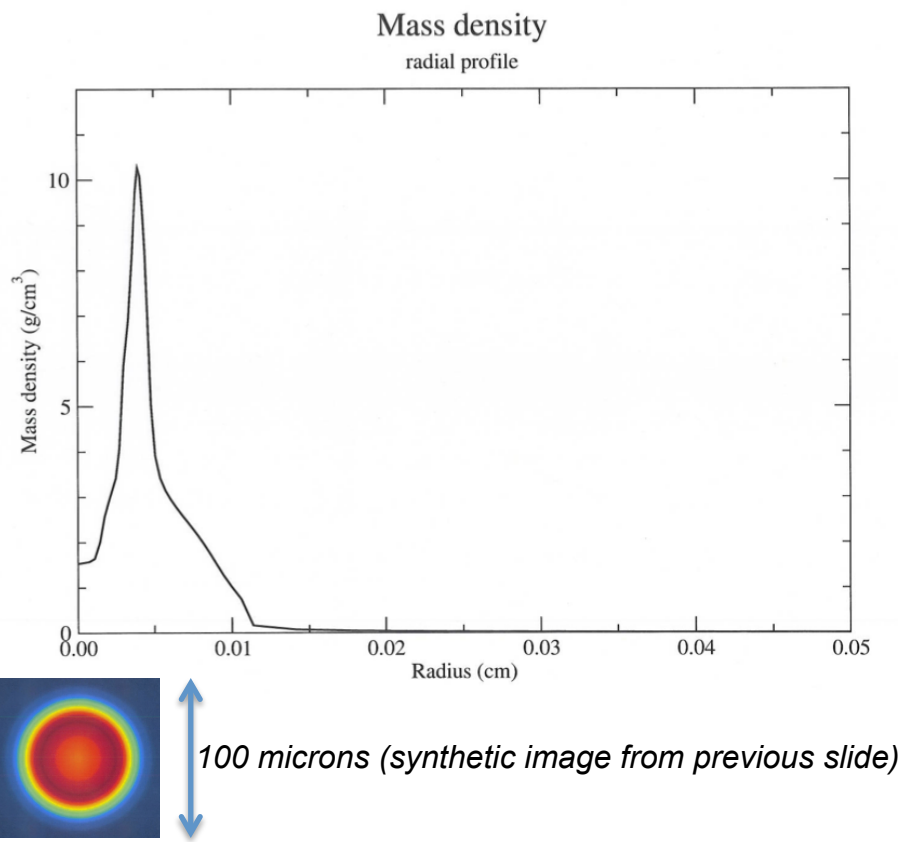
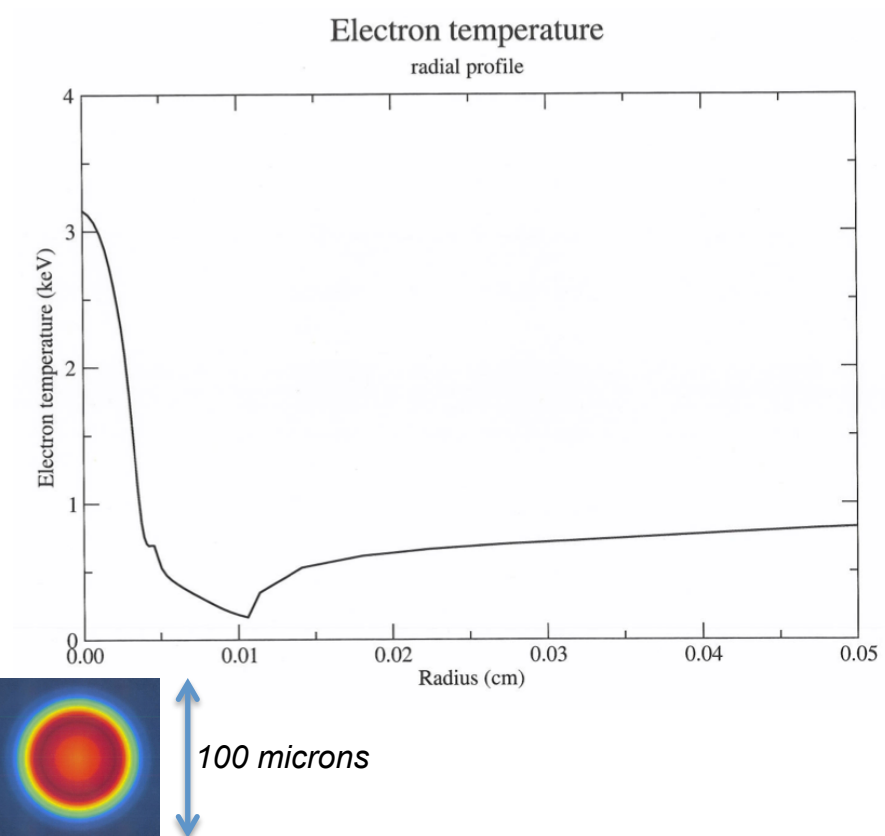
Synthetic image for band 2.9 - 4.5 keV



- 3-D raytracing (spherical shells, polygons, ...)
- NLTE EOS/spectral database from ATOMIC

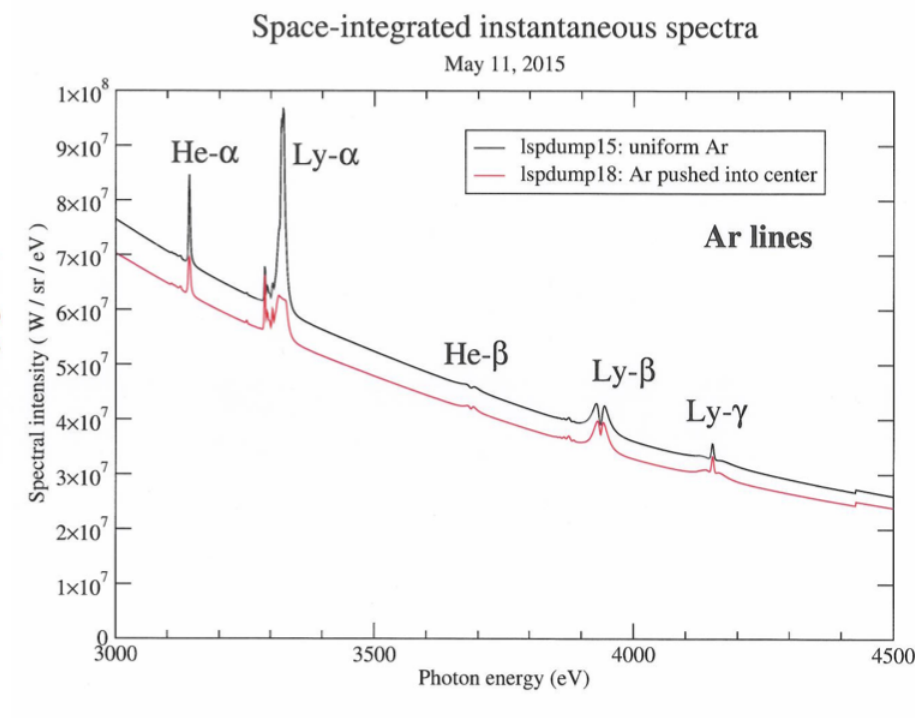
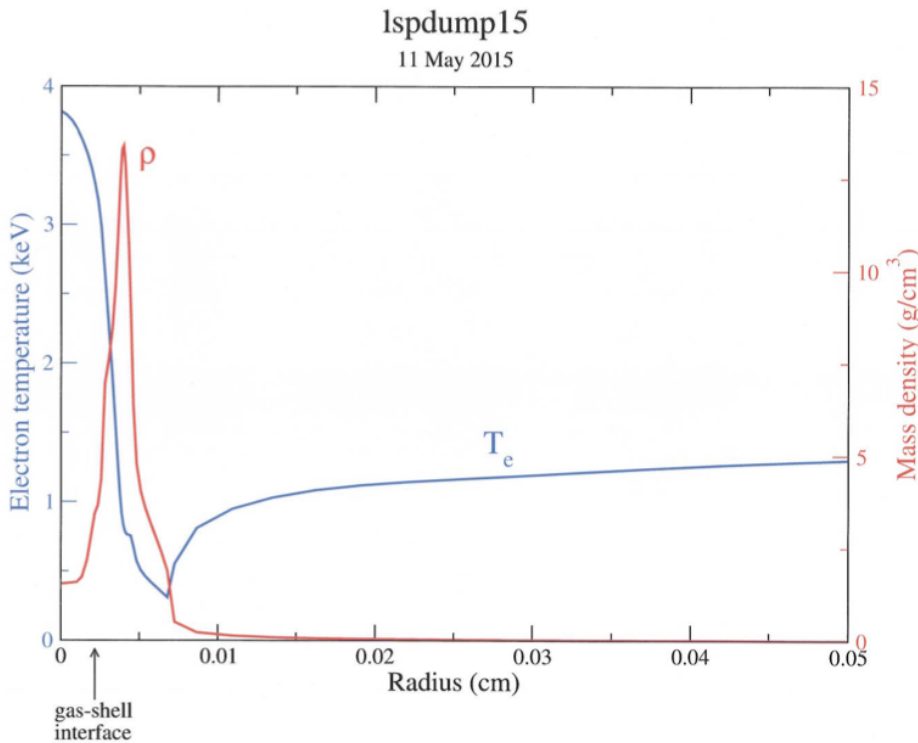
*Calculations were performed using parallel rays spaced 0.0001 cm (1 micron).*

# Hydra 1-D radial profiles input into FESTR



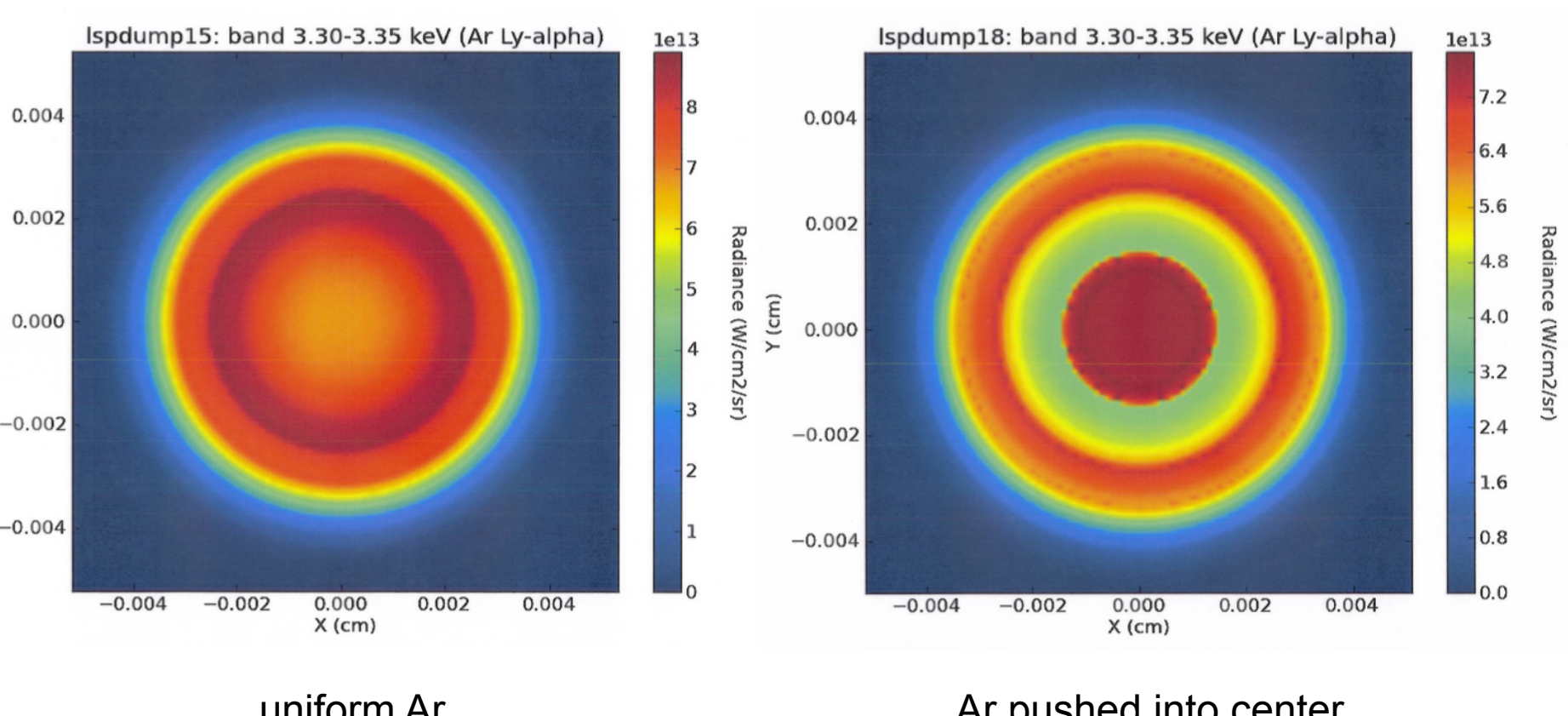
- 79 concentric spherical zones up to  $R = 0.24 \text{ cm}$
- Two materials:
  - gas fill: D 99%, Ar 1% ( $0 \text{ cm} < R < 0.0025 \text{ cm}$ )
  - shell: C 42%, H 55%, O 2%, N 1%

# Hydra 1-D profiles postprocessed by FESTR



- 79 concentric spherical zones up to  $R = 0.24$  cm
- Two materials:
  - gas fill: D 99%, Ar 1% ( $0 \text{ cm} < R < 0.0025 \text{ cm}$ ); **Ar pushed inward in lspdump18**
  - shell: C 50%, H 50%

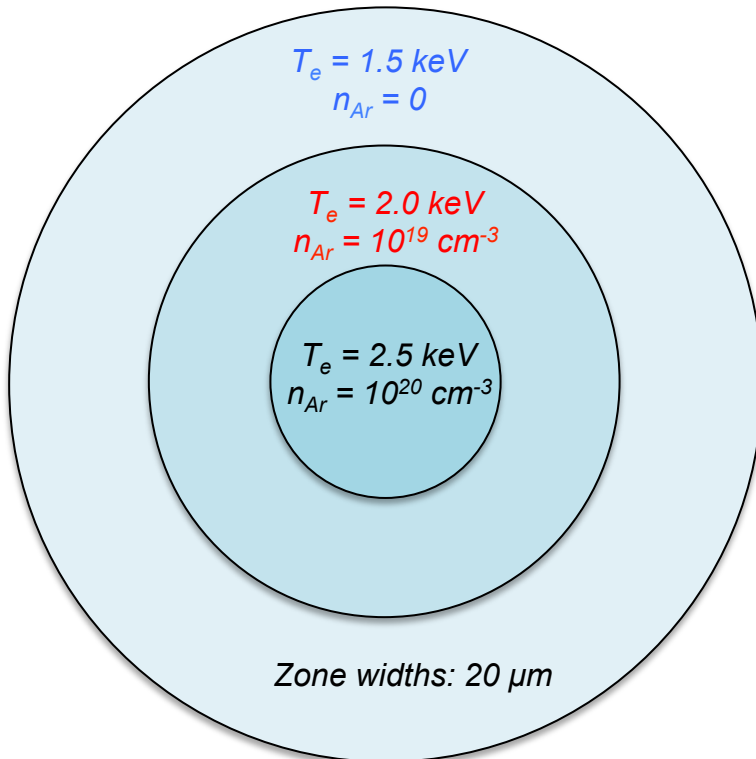
# Enhanced emission at center from separated Ar



We plan to compare such synthetic images with experimental data reconstructed from MMI measurements.

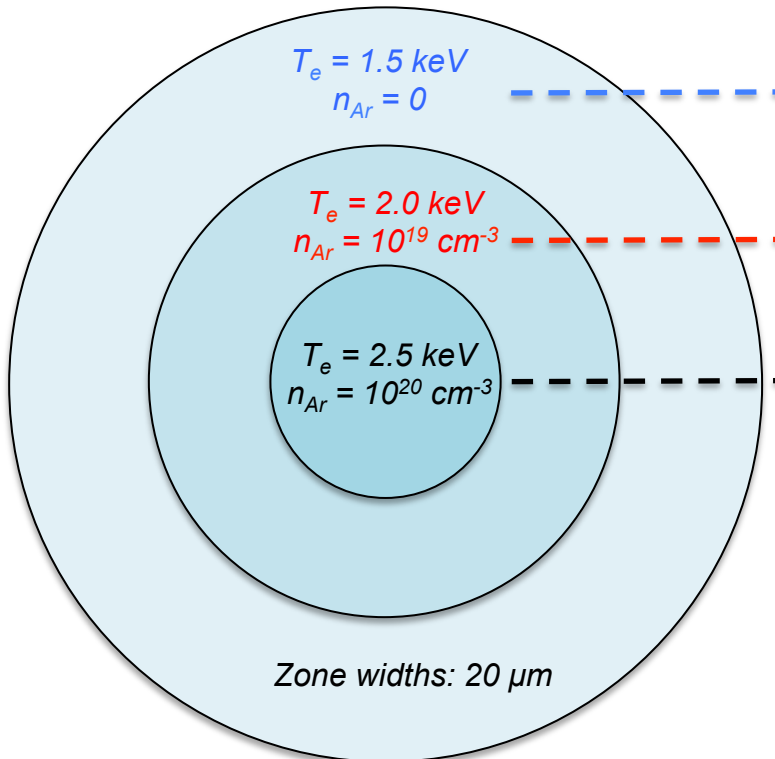
# Prototype of data analysis and reconstruction

---

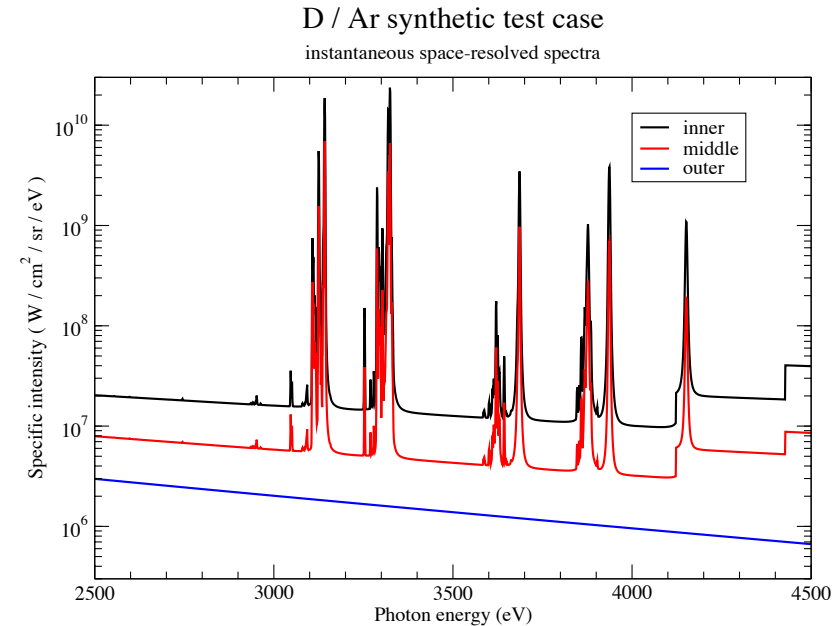


$n_D = 10^{22} \text{ cm}^{-3}$  everywhere

# Prototype of data analysis and reconstruction

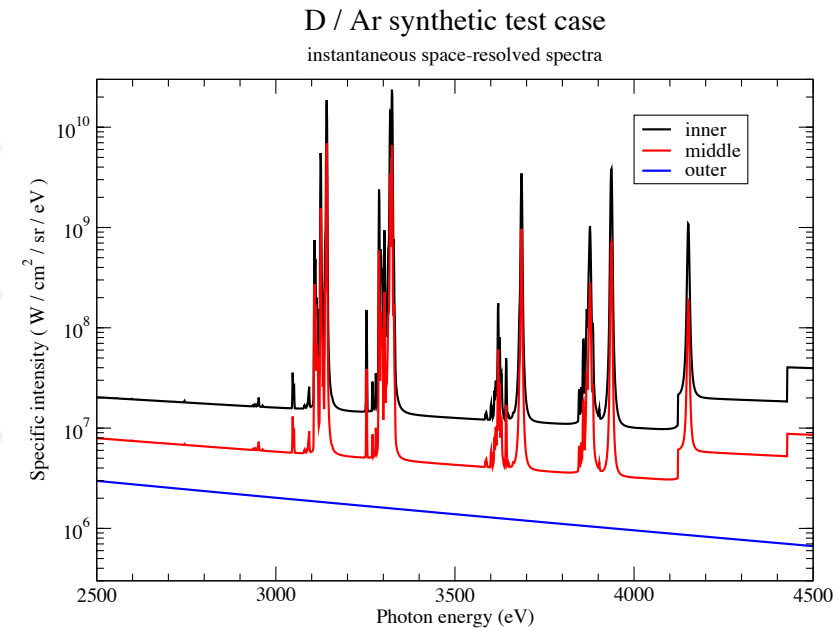
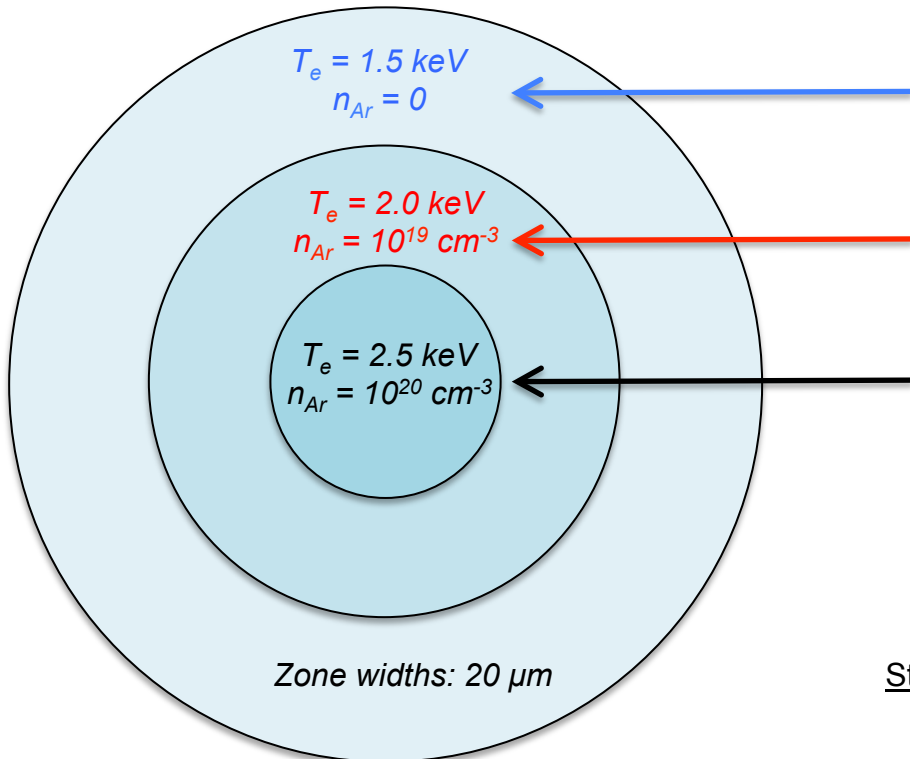


$n_D = 10^{22} \text{ cm}^{-3}$  everywhere



Step 1: FESTR in **postprocessing** mode generates space-resolved synthetic spectra from adopted target conditions.

# Prototype of data analysis and reconstruction



Step 1: FESTR in **postprocessing** mode generates space-resolved synthetic spectra from adopted target conditions.

Step 2: FESTR in **analysis** mode searches the parameter space and recovers adopted target conditions by matching spectra from Step 1.

# Outline

---

- Motivation
- Implementation
- Examples
- Future work

# Future work

---

- Parallelization, threading, vectorization, ...
- Write EnSight-based translators for various hydrocodes
- Add generalizations, use fewer approximations
  - Doppler shifts, molecular opacities, mixing of cold (neutral) materials, finite speed of light, scattering, ...
- Reverse the roles of inputs and outputs for analysis and reconstruction
  - account for: noise, resolution, size of parameter space, ...